Available online at www.sciencedirect.com
ScienceDirect
CRYOBIOLOGY
ELSEVIER
Cryobiology 53 (2006) 279–282
www.elsevier.com/locate/ycryo

Brief communication

Improvement in the long-term stability of freeze-dried mouse spermatozoa by adding of a chelating agent

Takehito Kaneko *, Naomi Nakagata

Division of Reproductive Engineering, Center for Animal Resources and Development (CARD), Kumamoto University, Kumamoto 860-0811, Japan

Received 1 March 2006; accepted 9 June 2006
Available online 25 July 2006

Abstract

This study demonstrates that a small amount of chelating agent in the freeze-drying solution is necessary to prevent the deterioration of spermatozoa during freeze-drying and subsequent preservation at 4 °C. We freeze-dried mouse epididymal spermatozoa in the solutions containing Tris–HCl and ethylenediaminetetraacetic acid (EDTA) as a chelating agent. Spermatozoa stored for various times up to 1 year at 4 °C were injected intracytoplasmically into individual oocytes, and the normality of chromosomes in fertilized oocytes was analyzed. In addition, embryos derived from freeze-dried spermatozoa were transferred into recipients to determine their developmental ability. Chromosomes were maintained well when spermatozoa were freeze-dried in a solution containing 10 mM Tris–HCl and 1 mM EDTA (73%), and 57% of embryos developed to term. Of embryos derived from spermatozoa stored for 1 year, 65% developed into live offspring. On the other hand, when spermatozoa were freeze-dried in a solution containing 10 mM Tris–HCl and 0 or 50 mM EDTA, spermatozoa that maintained karyotypically normal chromosomes were 64% or 22%, and only 16% or 3% of embryos were developed to term, respectively. This finding suggested that mouse spermatozoa can be freeze-dried in a simple solution containing the same composition as that used to preserve extracted DNA.

Keywords: Mouse; Spermatozoa; Freeze-drying; Preservation; Intracytoplasmic sperm injection; Fertilization; Low temperature

The sperm freeze-drying technique [12] is now becoming a new preservation method for the maintenance of genetic resources. An advantage of sperm freeze-drying is that it requires neither liquid nitrogen nor dry ice for the preservation and transportation of spermatozoa. Present freeze-drying solution containing 10 mM Tris–HCl, 50 mM NaCl, and 50 mM ethylene glycol-bis (β-aminoethyl ether)-*N*,*N*,*N*′,*N*′-tetraacetic acid (EGTA) [2] adjusted to pH 8.0 [3] is widely applied not only to the freeze-drying of epididymal spermatozoa [13,4,5] but also testicular spermatozoa [6]. Moreover, it is known that freeze-dried spermatozoa have been preserved without remarkable deterioration for periods of up to 1.5 years at 4 °C [13,4]. However, more consideration in order to increase the rate of success and long-term preservation of freeze-dried spermatozoa is needed. Although, ethylenediaminetetraacetic acid

* Corresponding author. Fax: +81 96 373 6570.
E-mail address: take@kumamoto-u.ac.jp (T. Kaneko).

0011-2240/$ - see front matter © 2006 Elsevier Inc. All rights reserved.
doi:10.1016/j.cryobiol.2006.06.004

(EDTA) is known as an alternative to EGTA as a chelating agent, the effect of EDTA on spermatozoa during freeze-drying and preservation has not been described. Here, we studied the necessity of chelating agent for the freeze-drying of mouse spermatozoa using EDTA.

The freeze-drying of spermatozoa was carried out using the procedure described previously [2,3,13,4]. The freeze-drying solution for spermatozoa contained 10 mM Tris–HCl and 0, 1, or 50 mM EDTA. The freeze-drying solution was adjusted to pH 8.0 by adding 1 M HCl [3,4], and it was then filter-sterilized and stored at 4 °C for less than 1 week before use. Each 1 ml of the freeze-drying solution was warmed to 37 °C in a 1.5 ml polypropylene microcentrifuge tube. Two cauda epididymides of the B6D2F1 hybrid male mouse were removed using a pair of small scissors. A dense mass of spermatozoa was squeezed out of each epididymis using sharply pointed forceps, and was then put gently on the bottom of the freeze-drying solution in the microcentrifuge tube. The sperm suspension was left at 37 °C for 10 min to allow the spermatozoa to disperse into the solution. The 800-μl supernatant was collected, and eight 100-μl aliquots were then placed into a long-necked glass ampoule for freeze-drying (651506, Wheaton, Millville, NJ). Ampoules were plunged into liquid nitrogen for 20 s, and were then connected with a freeze-drying machine (Freeze-drying systems 77530, Labconco, Kansas City, MO) under pressure at 39×10^{-3} to 45×10^{-3} hPa. All ampoules were flame-sealed after 4 h of drying and preserved at 4 °C for times of fewer than 7 days, 1 month, 3 months, or 1 year.

The medium used for oocyte manipulation was H-CZB medium, which is a modification of CZB medium [1] created by adding 20 mM Hepes-Na, 5 mM $NaHCO_3$, and 0.1 mg/ml polyvinyl alcohol instead of bovine serum albumin [7].

Superovulation was induced in B6D2F1 hybrid females for collecting oocytes by an intraperitoneal injection of 7.5 IU PMSG (Teikokuzoki Co., Tokyo, Japan) followed by an injection of 7.5 IU hCG (Teikokuzoki Co.) 48 h later. Cumulus-oocyte complexes were collected from oviducts 13–15 h after the hCG injection. Oocytes were freed from cumulus cells by treatment with 0.1% hyaluronidase in H-CZB medium.

Sperm injection was carried by the method previously described by Kimura and Yanagimachi [7] with minor modifications. Freeze-dried spermatozoa in the ampoule were rehydrated by adding 100-μl of sterile distilled water. A small volume (1 to 2-μl) of the sperm suspension was mixed thoroughly with a droplet of H-CZB medium containing 12% (w/v) polyvinylpyrrolidone (ICN Pharmaceuticals, Costa Mesa, CA). A single spermatozoon that showed a normal shape was drawn from the tail into the injection pipette. The sperm head was separated from the tail by applying a few piezo-pulses when the junction between the head and tail was at the opening of the pipette. Only sperm heads were injected immediately into each oocyte. The oocytes after sperm injection were cultured in CZB medium supplemented with 5.56 mM D-glucose (m-CZB) at 37 °C under 5% CO_2 and 95% air.

The oocytes appeared two distinct pronuclei and a second polar body at 5 h after sperm injection was recorded as fertilized. Chromosomes of fertilized oocytes were analyzed using the method described previously [8]. Briefly, fertilized oocytes were cultured in m-CZB medium containing 0.006 μg/ml vinblastine to arrest oocytes at the metaphase of the first cleavage. After 19–21 h of culture, arrested oocytes were treated for 5 min with 0.5% pronase (Kaken Pharmaceuticals, Tokyo, Japan) in phosphate buffer saline (pH 7.4) to remove the zona pellucida, and transferred to the hypotonic solution (1:1 mixture of 30% fetal bovine serum and 1% sodium citrate) for 5 min. Oocytes were then fixed and air-spread on a glass slide, and their chromosomes were assessed by Giemsa staining. An oocyte with two groups of 20 chromosomes without any structural and numerical abnormalities was recorded as karyotypically normal. When more than 10 chromosome breaks were observed in one group of chromosomes, oocytes were recorded as having multiple aberrations. Oocytes were recorded as having minor aberrations if less than nine chromosome breaks were observed in one group of chromosomes.

Fertilized oocytes were cultured in m-CZB medium until they developed to the 2-cell stage. At 22–24 h after sperm injection, 7–20 of the 2-cell embryos were transferred into the oviducts of each recipient CD1 female that had been mated with a vasectomized male of the same strain on the day before embryo transfer. Numbers of implantation sites and normal live offspring were assessed on day 19.5 of gestation.

All data obtained from this study were compared by a chi-square test using Yates correction for continuity.

The rate of spermatozoa that maintained normal chromosomes were 64% or 73% when freeze-dried in

the solution containing 10 mM Tris–HCl and 0 or 1 mM EDTA, respectively (Table 1). However, only 22% of spermatozoa that were freeze-dried in the solution containing 10 mM Tris–HCl and 50 mM EDTA were capable of maintaining normal chromosomes ($p < 0.005$), and the number of oocytes with multiple chromosomal aberrations increased. In all solutions with different concentrations of EDTA, shown in Table 2, a high proportion of oocytes after ICSI survived (>70%), were fertilized (>92%) and developed to the 2-cell stage (>82%). And 57% of embryos with spermatozoa freeze-dried in the solution containing 10 mM Tris–HCl and 1 mM EDTA developed to normal term after transfer into oviducts of surrogate females. On the other hand, the development to term of embryos with spermatozoa freeze-dried in the solution containing 10 mM Tris–HCl and 0 or 50 mM EDTA was only 16% or 3% ($p < 0.005$), respectively. The spermatozoa that were freeze-dried in the solution containing 10 mM Tris–HCl and 1 mM EDTA were capable of being preserved completely 1 month, 3 month, and 1 year later at 4 °C, resulting in the development of 55%, 58%, and 65% of embryos being developed to normal term after transfer into the oviducts of surrogate females, respectively (Table 3).

This study demonstrated that chromosome integrity and the developmental ability of spermatozoa could be maintained well by adding a small amount of EDTA into the solution during freeze-drying and subsequent preservation. The novel observation of this study is that mouse spermatozoa

Table 1
Chromosome analysis of spermatozoa freeze-dried using solution with different concentration of EDTA[A]

Conc. of Tris–HCl (mM)	Conc. of EDTA (mM)	pH	No. of oocytes analyzed	No. of oocytes with multiple chromosomal aberrations	No. of oocytes with minor chromosomal aberrations	No. (%) [range] of oocytes with normal chromosomes[B]
10	0	8	66	2	22	42 (64) [60–68][a]
10	1	8	60	0	16	44 (73) [62–83][a]
10	50	8	81	19	44	18 (22) [0–32][b]

Percentages with different lower case superscript letters were significantly different ($p < 0.005$).
[A] Spermatozoa were preserved for less than 7 days.
[B] Percentage from no. of oocytes analyzed.

Table 2
Development of oocytes fertilized with spermatozoa freeze-dried using solution with different concentration of EDTA[A]

Conc. of EDTA (mM)[B]	No. of oocytes injected	No. (%) of oocytes survived[C]	No. of oocytes fertilized	No. of 2-cell embryos transferred	No. (%) of implantation site[D,E]	No. (%) [range] of live offspring[D]
0	135	94 (70)	91	84	32 (38)[a]	13 (16) [7–30][d]
1	150	109 (73)	100	91	62 (68)[b]	52 (57) [50–68][e]
50	198	149 (75)	142	116	10 (9)[c]	3(3) [0–7][f]

Percentages with different lower case superscript letters were significantly different ($p < 0.005$).
[A] Spermatozoa were preserved for less than 7 days.
[B] EDTA added in 10 mM Tris–HCl, and then adjusted to pH 8.0.
[C] Percentage from no. of oocytes injected.
[D] Percentage from no. of oocytes transferred.
[E] Implantation site = the number of resorption site + normal live offspring.

Table 3
Development of oocytes fertilized with freeze-dried spermatozoa preserved at 4 °C for a long periods of time[a]

Storage term	No. of oocytes injected	No. (%) of oocytes survived[b]	No. of oocytes fertilized	No. of 2-cell embryos transferred	No. (%) of implantation site[c,d]	No. (%) of live offspring[c]
1 month	46	24 (52)	23	20	13 (65)	11 (55)
3 month	100	55 (55)	51	47	33 (70)	27 (58)
1 year	104	79 (76)	76	63	54 (86)	41 (65)

[a] The solution containing 10 mM Tris–HCl and 1 mM EDTA adjusted to pH 8.0 were used.
[b] Percentage from no. of oocytes injected.
[c] Percentage from no. of oocytes transferred.
[d] Implantation site = the number of resorption site + normal live offspring.

can be successfully freeze-dried in a simple solution containing the same composition as that used to preserve extracted DNA. At present, freeze-drying solution contains a high concentration of EGTA (50 mM) and NaCl (50 mM) in 10 mM Tris–HCl [2,3,13,4–6]. When spermatozoa were freeze-dried in the solution containing 10 mM Tris–HCl and 1 mM EDTA, however, 73% of the spermatozoa had normal chromosomes without any structural and numerical abnormalities (Table 1). And 57% of embryos with these spermatozoa developed to normal term (Table 2). Moreover, live offspring were obtained from oocytes fertilized with spermatozoa stored for 1 year (Table 3).

Kaneko and Nakagata [4] reported that the preservation at a low temperature is important for the long-term stable preservation of freeze-dried spermatozoa. The chromosome integrity of freeze-dried spermatozoa preserved at less than 4 °C has been maintained completely, even during preservation for 17 months. Our study also showed that 4 °C is an optimal temperature for the preservation of freeze-dried spermatozoa, and results in more reliable long-term preservation than by methods previously reported [12,2,3,13,4,6]. Preservation at 4 °C is more advantageous economically for long-term preservation, and allow for simpler transportation than at −20 °C or lower.

The high concentration of EGTA is also an important component as chelating agents, since it defines the ability of chelating agents to suppress endonuclease activity during preservation [2]. The results of our study show that EDTA had the same effect as EGTA (Table 1). It is thought that a chelating agent such as EGTA and EDTA was necessary to protect spermatozoa from damage by freeze-drying. Furthermore, our results demonstrated clearly that EDTA prevented the fragmentation of sperm chromosomes more efficiently by an amount less than EGTA during freeze-drying and subsequent preservation.

In this study, the preservation of freeze-dried spermatozoa at 4 °C for long periods of time was archived by use of a solution containing 10 mM Tris–HCl and 1 mM EDTA adjusted to pH 8.0. Cryopreserved spermatozoa need a constant supply of liquid nitrogen for preservation and transportation. However, the achievement of long-term preservation and shipment of freeze-dried spermatozoa would obviate the processes of preparation of liquid nitrogen [9], vapor shipper containers [10], or dry ice [11] that are required for cryopreserved spermatozoa. We aim to establish the freeze-drying method as a convenient tool in which simple preservation and shipment are possible.

References

[1] C.L. Chatot, C.A. Ziomek, B.D. Bavister, J.L. Lewis, I. Torres, An improved culture medium supports development of random-bred 1-cell mouse embryos in vitro, J. Reprod. Fertil. 86 (1989) 679–688.
[2] H. Kusakabe, M.A. Szczygiel, D.G. Whittingham, R. Yanagimachi, Maintenance of genetic integrity in frozen and freeze-dried mouse spermatozoa, Proc. Natl. Acad. Sci. USA 98 (2001) 13501–13506.
[3] T. Kaneko, D.G. Whittingham, R. Yanagimachi, Effect of pH value of freeze-drying solution on the chromosome integrity and developmental ability of mouse spermatozoa, Biol. Reprod. 68 (2003) 136–139.
[4] T. Kaneko, N. Nakagata, Relation between storage temperature and fertilizing ability of freeze-dried mouse spermatozoa, Comp. Med. 55 (2005) 140–144.
[5] Y. Kawase, H. Araya, N. Kamada, K. Jishage, H. Suzuki, Possibility of long-term preservation of freeze-dried mouse spermatozoa, Biol. Reprod. 72 (2005) 568–573.
[6] T. Kaneko, D.G. Whittingham, J.W. Overstreet, R. Yanagimachi, Tolerance of the mouse sperm nuclei to freeze-drying depends on their disulfide status, Biol. Reprod. 69 (2003) 1859–1862.
[7] Y. Kimura, R. Yanagimachi, Intracytoplasmic sperm injection in the mouse, Biol. Reprod. 52 (1995) 709–720.
[8] Y. Kamiguchi, K. Mikamo, An improved, efficient method for analyzing human sperm chromosomes using zona-free hamster ova, Am. J. Hum. Genet. 38 (1986) 724–740.
[9] N. Nakagata, Cryopreservation of mouse spermatozoa, Mamm. Genome 11 (2000) 572–576.
[10] A. Nagy, M. Gertsenstein, K. Vintersten, R. Behringer, Cryopreservation, Rederivation, and Transport of Mice, Manipulating the Mouse Embryo, A Laboratory Manual, third ed., Cold Spring Harbor Laboratory Press, New York, 2003, 599–628.
[11] M. Okamoto, N. Nakagata, Y. Toyoda, Cryopreservation and transport of mouse spermatozoa at −79 °C, Exp. Anim. 50 (2001) 83–86.
[12] T. Wakayama, R. Yanagimachi, Development of normal mice from oocytes injected with freeze-dried spermatozoa, Nat. Biotechnol. 16 (1998) 639–641.
[13] M.A. Ward, T. Kaneko, H. Kusakabe, J.D. Biggers, D.G. Whittingham, R. Yanagimachi, Long-term preservation of mouse spermatozoa after freeze-drying and freezing without cryoprotection, Biol. Reprod. 69 (2003) 2100–2108.

Available online at www.sciencedirect.com
ScienceDirect
Theriogenology
ELSEVIER
Theriogenology 66 (2006) 1098–1101
www.journals.elsevierhealth.com/periodicals/the

Long-term cryopreservation of mouse sperm

Takehito Kaneko, Ayako Yamamura, Yukie Ide, Mami Ogi, Tomoko Yanagita, Naomi Nakagata *

Division of Reproductive Engineering, Center for Animal Resources and Development (CARD), Kumamoto University, 2-2-1 Honjo, Kumamoto 860-0811, Japan

Received 27 December 2005; accepted 18 February 2006

Abstract

The objective was to determine if mouse sperm can maintain their fertilizing ability after being frozen for >10 y and whether the offspring derived from these sperm had normal fertilizing ability and phenotype. We cryopreserved sperm from six strains of mice (C57BL/6J, DBA/2N, BALB/cA, C3H/HeJ, B6D2F1 and B6C3F1) in a solution containing 18% (w/v) raffinose and 3% (w/v) skim milk, and preserved them in liquid nitrogen for >10 y. To assess the normality and fertilizing ability of these sperms, they were thawed and used for in vitro fertilization of oocytes of the same strains. Fertilization rates for C57BL/6J, DBA/2N, BALB/cA, C3H/HeJ, B6D2F1 and B6C3F1 were 66.4, 92.3, 72.8, 32.9, 60.3 and 53.7%, respectively. Furthermore, 38.3, 15.0, 43.3, 26.1, 38.3 and 16.7% of the embryos transferred to pseudopregnant females developed and produced live offspring that had normal phenotype and fertility.

Keywords: Mouse; Cryopreservation; Sperm; Fertilization; Embryo

1. Introduction

Successful cryopreservation of murine sperm was reported in the 1990s [1–6]. Subsequent improvements of cryopreservation methods have increased success [7] and high fertilization rates can be obtained using sperm frozen in a solution containing 18% (w/v) raffinose and 3% (w/v) skim milk. Moreover, this cryopreservation method was also applied to various strains [8], wild mice [9] and transgenic mice [10].

In recent years, several large mouse sperm/embryo cryobanks have been established at various locations around the world. The sperm of numerous transgenic, knockout and mutant mouse strains have been cryopreserved on a large-scale. Although the fertilizing ability of sperm from other species was not affected by long-term cryopreservation [11–16], doubts still exist as to whether mouse sperm can maintain their fertilizing ability after long-term cryopreservation. To clarify the situation, we studied the normality and fertilizing ability of sperm that had been cryopreserved for >10 y. In this study, six strains of frozen–thawed sperm were used and fertility in vitro and subsequent development of the fertilized oocytes was assessed.

2. Materials and methods

2.1. Animals

All mice were purchased from CLEA Japan, Inc. (Tokyo, Japan). Six strains (C57BL/6J, DBA/2N, BALB/cA, C3H/HeJ, B6D2F1 and B6C3F1) were used for this study. The males and female mice used for sperm and oocyte donation were >11 and 8–12 wk old,

* Corresponding author. Tel.: +81 96 373 6570; fax: +81 96 373 6570.
E-mail address: nakagata@kumamoto-u.ac.jp (N. Nakagata).

0093-691X/$ – see front matter © 2006 Elsevier Inc. All rights reserved.
doi:10.1016/j.theriogenology.2006.02.049

respectively. Mice used as recipients for the transfer of two-cell embryos were from the ICR strain, 8–16 wk old. All animals were maintained in an air-conditioned (22 ± 1 °C) and light-controlled room (lights on from 07:00 to 19:00 h). The Animal Care and Use Committee of the Kumamoto University School of Medicine approved all procedures performed in this study.

2.2. Media

For preparation of the sperm cryopreservation solution, 18% (w/v) raffinose (180-00012, Wako Pure Chemical Industries, Ltd., Osaka, Japan) and 3% (w/v) skim milk (232100, Difco, Sparks, MD, USA) were mixed with 50 mL of sterile distilled water (W1503, Sigma, St. Louis, MO, USA) in a 50 mL conical tube (2070, Falcon, Franklin Lakes, NJ, USA). The mixture was left at 60 °C in a water bath for 1 h and then 1.5 mL of the mixture was transferred to a 1.5 mL polypropylene micro-centrifuge tube that was centrifuged at 10,000 × *g* for 15 min at room temperature. The supernatant was collected and filtered with a 0.45 μm disposable filter unit (SLHV025LS, Millipore Co., Bedford, MA, USA), put into 1 mL glass ampoules, flame-sealed, and stored at room temperature. HTF medium [17] was used for oocyte collection and in vitro fertilization.

2.3. Sperm collection and cryopreservation

Sperm cryopreservation was carried out as described by Nakagata and Takeshima [7]. Four cauda epididymides from two males of each strain were collected using sharp scissors. Blood and adipose tissue were removed and the epididymides were transferred to 400 μL of cryopreservation solution in four-well multi-dishes (176740, Nunc A/S, Roskilde, Denmark). Each epididymis was well minced using micro-spring scissors and the sperm in the solution were dispersed by gently shaking the dish for 2 min. Aliquots of sperm suspension (100 μL) were loaded into 0.25 mL sampling straws (005565, IMV Technologies, L'Aigle Cedex, France). These straws were heat-sealed at both ends and cooled in gas phase of about 1 cm above liquid nitrogen for 15 min, and then plunged directly into the liquid nitrogen. All sperm used in this investigation were frozen between December 2, 1991 and August 10, 1993.

2.4. Sperm thawing and in vitro fertilization

The frozen sperm were thawed between October 9, 2003 and January 22, 2004 by immersion in a water bath (37 °C) for 15 min. The sperm suspension was pushed out of the straw into a plastic dish and diluted with 1.9 mL of HTF medium. The sperm suspension was aspirated into a 2 mL syringe, and a 0.45 μm disposable filter unit was attached to the end of the syringe. The sperm suspension was slowly filtered to remove the cryopreservation solution, followed by aspiration of 2 mL of fresh HTF medium through the filter. The sperm suspension was again slowly filtered. Finally, a 200 μL drop of the sperm suspension was formed in a culture dish covered with paraffin oil (26137-85, Nacalai Tesque, Inc., Kyoto, Japan) and incubated for 1 h at 37 °C in 5% CO_2 and 95% air.

Oocytes were collected from superovulated females of each strain. Superovulation was induced by 5 IU of PMSG (Teikokuzoki Co., Tokyo, Japan) given IP, followed by 5 IU of hCG (Teikokuzoki Co.) IP 48 h later. Cumulus–oocyte complexes were collected from oviducts 13–15 h after hCG and were introduced directly into a 200 μL drop of sperm suspension that had been incubated for 1 h [7]. The sperm and oocytes were incubated at 37 °C in 5% CO_2 and 95% air.

2.5. Embryo transfer

Twenty-four hours after insemination, embryos that had developed to the two-cell stage were randomly selected for embryo transfer. Pseudopregnant ICR females that had been mated with vasectomized males of the same strain 1 d before embryo transfer were used as recipients. For each strain of mice, 14–20 two-cell embryos were transferred into the oviducts of three pseudopregnant recipients. Offspring that were born naturally after 19.5 d of gestation were fostered. The offspring were raised to maturity and within-strain matings were done to assess fertilizing ability.

2.6. Phenotypic analysis

Six males and six females derived from the frozen–thawed C57BL/6J sperm were selected at random for phenotype analysis. At 7–10 wk of age, these mice were subjected to a phenotypic analysis, including general observation, body weight measurements, motor coordination tests (rotarod test), learning and memory tests (multiple T swim maze performance test), urinalysis (pH, protein, glucose and occult blood), locomotor activity tests (open field test), complete blood counts, blood biochemistry, functional observational battery (FOB) tests, autopsy, organ weight measurements and histopathological examination. The data were compared statistically with C57BL/6J derived from standard breeding colonies (purchased from CLEA, Japan).

Table 1
Fertilizing ability of mouse sperm cryopreserved for >10 y and used for in vitro fertilization of oocytes derived from the same strain

Strain of origin	No. of oocytes examined	No. of oocytes that developed to the two-cell stage (%)
C57BL/6J	140	93 (66.4)[abc]
DBA/2N	366	338 (92.3)[d]
BALB/cA	243	177 (72.8)[be]
C3H/HeJ	140	46 (32.9)[f]
B6D2F1	436	263 (60.3)[cgh]
B6C3F1	363	195 (53.7)[hi]

Within a column, percentages with different lower case superscript letters (a–i) were different ($P < 0.05$).

2.7. Analysis of data

The Chi-square test using Yate's correction for continuity was used for analysis of data obtained from the fertilizing ability of frozen–thawed sperm and the subsequent development of embryos. Student's *t*-test was used for the data of phenotypic analysis between C57BL/6J mice derived from frozen–thawed sperm and mice derived from standard breeding colonies.

3. Results

The fertilizing ability of sperm from each strain that was cryopreserved for >10 y is shown in Table 1. In all strains, oocytes were fertilized by frozen–thawed sperm and these fertilized oocytes developed to the two-cell stage. Although the number of two-cell embryos that developed to term differed among strains, both male and female offspring were obtained in all strains (Table 2). These offspring had normal fertility; normal pups were obtained from three pairs of each strain selected at random. In DBA/2N, three females were mated with the same male, because only one male was obtained (Table 2). There were no significant phenotypic differences between C57BL/6J mice derived from frozen–thawed sperm and mice derived from standard breeding colonies.

4. Discussion

In this study, fertilizing ability of mouse sperm were maintained during long-term cryopreservation in liquid nitrogen. Furthermore, the fertility of the offspring derived from these frozen–thawed sperm was not impaired and there were no significant differences between mice derived from frozen–thawed sperm and mice derived from standard breeding colonies. This is apparently the first report documenting the normality of mouse sperm after long-term cryopreservation.

Regarding the relationship between storage temperature and the period of sperm preservation, we reported that mouse sperm stored at −80 °C had reduced fertilizing ability after 8 mo of storage [18]. Conversely, in other species, long-term storage at −196 °C had no influence on the fertilizing ability of sperm [11–16]. Based on these reports (including our present study), storage at −196 °C is the most appropriate for the long-term storage of sperm.

Over the past 20 y, many new mouse strains (e.g. transgenic, knockout and induced mutations) have been produced worldwide. Consequently, the number of novel mouse strains has expanded rapidly, and the maintenance of these strains by standard breeding colonies is becoming increasingly difficult [19]. In general, embryo freezing is a well-established procedure [20] and is probably the most reliable means for banking mouse models of major importance. However, embryo freezing requires considerable skill and a large number of mice to provide sufficient embryos (over 500 embryos/strain) [21]. In contrast, sperm freezing is relatively simple, rapid and economical. A large number of sperm ($1–3 \times 10^7$) can be frozen immediately after collection from each male and many animals can be produced from one aliquot of frozen sperm [22]. The freezing method used in the present study was not only

Table 2
Development of murine oocytes fertilized in vitro with sperm of the same strain that had been cryopreserved for >10 y

Strain of origin	No. of embryos transferred	No. of recipients	No. of offspring (%)	Sex of offspring	
				No. of males	No. of females
C57BL/6J	60	3	23 (38.3)[ab]	13	9
DBA/2N	60	3	9 (15.0)[cd]	1	8
BALB/cA	60	3	26 (43.3)[ab]	8	18
C3H/HeJ	46	3	12 (26.1)[bd]	5	7
B6D2F1	60	3	23 (38.3)[ab]	12	11
B6C3F1	60	3	10 (16.7)[cd]	4	6

Within a column, percentages with different lower case superscript letters (a–d) were different ($P < 0.05$).

adopted for the large-scale sperm preservation project in the cryobank [22–24], but also played a big role in the large-scale screening of new mutant mouse lines generated by treatment with *N*-ethyl-*N*-nitrosourea (ENU) [25,26].

In this study, fertilizing ability had strain-dependent susceptibility to damage by freezing [22,23]. However, even if the fertilizing ability of the frozen–thawed sperm is low, these sperm are suitable for assisted fertilization techniques such as partial zona dissection before insemination in vitro [27]. Moreover, even in cases where the frozen sperm are immotile after thawing, oocytes can be fertilized via intracytoplamic sperm injection (ICSI) [28]. Therefore, we believe strongly that in the near future sperm freezing will become the preferred methods for maintenance of mouse strains as genetic resources.

References

[1] Okuyama M, Isogai S, Saga M, Hamada H, Ogawa S. In vitro fertilization (IVF) and artificial insemination (AI) by cryopreserved spermatozoa in mouse. J Fertil Implant 1990;7:116–9.

[2] Tada N, Sato M, Yamanoi J, Mizorogi T, Kasai K, Ogawa S. Cryopreservation of mouse spermatozoa in the presence of raffinose and glycerol. J Reprod Fertil 1990;89:511–6.

[3] Yokoyama M, Akiba H, Katsuki M, Nomura T. Production of normal young following transfer of mouse embryos obtained by in vitro fertilization using cryopreserved spermatozoa. Exp Anim 1990;39:125–8.

[4] Takeshima T, Nakagata N, Ogawa S. Cryopreservation of mouse spermatozoa. Exp Anim 1991;40:493–7.

[5] Penfold LM, Moore HD. A new method for cryopreservation of mouse spermatozoa. J Reprod Fertil 1993;99:131–4.

[6] Songsasen N, Betteridge KJ, Leibo SP. Birth of live mice resulting from oocytes fertilized in vitro with cryopreserved spermatozoa. Biol Reprod 1997;56:143–52.

[7] Nakagata N, Takeshima T. High fertilizing ability of mouse spermatozoa diluted slowly after cryopreservation. Theriogenology 1992;37:1283–91.

[8] Nakagata N, Takeshima T. Cryopreservation of mouse spermatozoa from inbred and F1 hybrid strains. Exp Anim 1993;42:317–20.

[9] Nakagata N, Ueda S, Yamanouchi K, Okamoto M, Matsuda Y, Tsuchiya K, et al. Cryopreservation of wild mouse spermatozoa. Theriogenology 1995;43:635–43.

[10] Nakagata N. Use of cryopreservation techniques of embryos and spermatozoa for production of transgenic (Tg) mice and for maintenance of Tg mouse lines. Lab Anim Sci 1996;46:236–8.

[11] Horne G, Atkinson AD, Pease EH, Logue JP, Brison DR, Lieberman BA. Live birth with sperm cryopreserved for 21 years prior to cancer treatment: case report. Hum Reprod 2004;19:1448–9.

[12] Leibo SP, Songsasen N. Cryopreservation of gametes and embryos of non-domestic species. Theriogenology 2002;57:303–26.

[13] Leibo SP, Semple ME, Kroetsch TG. In vitro fertilization of oocytes by 37-year-old cryopreserved bovine spermatozoa. Theriogenology 1994;42:1257–62.

[14] Salamon S, Maxwell WM. Storage of ram semen. Anim Reprod Sci 2000;62:77–111.

[15] Krause HD, Sieme H, Merkt H, Bader H, Wockener A. Successful use of deep-frozen stallion sperm after 23 years of storage at −196 °C. Dtsch Tierarztl Wochenschr 1990;97:544–5.

[16] Kozumplik J. Qualitative changes and the fertilizing capacity of sperm after 6 years of preservation of boar semen. Vet Med 1985;30:289–300.

[17] Quinn P, Kerin JF, Warnes GM. Improved pregnancy rate in human in vitro fertilization with the use of a medium based on the composition of human tubal fluid. Fertil Steril 1985;44:493–8.

[18] Okamoto M, Nakagata N, Toyoda Y. Cryopreservation and transport of mouse spermatozoa at −79 °C. Exp Anim 2001;50:83–6.

[19] Knight J, Abbott A. Full house. Nature 2002;417:785–6.

[20] Whittingham DG, Leibo SP, Mazur P. Survival of mouse embryos frozen to −196 °C and −269 °C. Science 1972;178:411–4.

[21] Mobraaten L. The Jackson Laboratory genetics stocks resource repository. In: Zeilmaker GH, editor. Frozen storage of laboratory animals. Stuttgart, NY: Gustav Fischer Verlag; 1981 p. 165–77.

[22] Nakagata N. Cryopreservation of mouse spermatozoa. Mamm Genome 2000;11:572–6.

[23] Sztein JM, Farley JS, Mobraaten LE. In vitro fertilization with cryopreserved inbred mouse sperm. Biol Reprod 2000;63:1774–80.

[24] Glenister PH, Thornton CE. Cryoconservation—archiving for the future. Mamm Genome 2000;11:565–71.

[25] Marschall S, Huffstadt U, Balling R, Hrabe de Angelis M. Reliable recovery of inbred mouse lines using cryopreserved spermatozoa. Mamm Genome 1999;10:773–6.

[26] Thornton CE, Brown SD, Glenister PH. Large numbers of mice established by in vitro fertilization with cryopreserved spermatozoa: implications and applications for genetic resource banks, mutagenesis screens, and mouse backcrosses. Mamm Genome 1999;10:987–92.

[27] Nakagata N, Okamoto M, Ueda O, Suzuki H. Positive effect of partial zona-pellucida dissection on the in vitro fertilizing capacity of cryopreserved C57BL/6J transgenic mouse spermatozoa of low motility. Biol Reprod 1997;57:1050–5.

[28] Sakamoto W, Kaneko T, Nakagata N. Use of frozen–thawed oocytes for efficient production of normal offspring from cryopreserved mouse spermatozoa showing low fertility. Comp Med 2005;55:136–9.

BIOLOGY OF REPRODUCTION 76, 303–313 (2007)
Published online before print 1 November 2006.
DOI 10.1095/biolreprod.106.054619

LGR4 Regulates the Postnatal Development and Integrity of Male Reproductive Tracts in Mice[1]

Takayuki Hoshii,[3] Toru Takeo,[4] Naomi Nakagata,[4] Motohiro Takeya,[5] Kimi Araki,[2] and Ken-ichi Yamamura[2,3]

Division of Developmental Genetics,[3] Institute of Molecular Embryology and Genetics, and Division of Reproductive Engineering,[4] Institute of Resource Development and Analysis, Kumamoto University, Kumamoto 860-0811, Japan
Department of Cell Pathology,[5] Kumamoto University School of Medicine, Kumamoto 860-8556, Japan

ABSTRACT

The roles of the leucine-rich repeat domain containing G protein-coupled receptor (GPCR) 4 (*Lgr4*), which is one of the orphan GPCRs, were analyzed with the *Lgr4* hypomorphic mutant mouse line ($Lgr4^{Gt}$). This homozygous mutant had only one-tenth the normal transcription level; furthermore, 60% of them survived to adulthood. The homozygous male was infertile, showing morphologic abnormalities in both the testes and the epididymides. In the testes, luminal swelling, loss of germinal epithelium in the seminiferous tubules, and rete testis dilation were observed. Cauda epididymidis sperm were immotile. Rete testis dilation was due to a water reabsorption failure caused by a decreased expression of an estrogen receptor (ESR1) and SLC9A3 in the efferent ducts. Although we found differential regulation of ESR1 expression in the efferent ducts and the epididymis, the role of ESR1 in the epididymis remains unclear. The epididymis contained short and dilated tubules and completely lacked its initial segment. In the caput region, we observed multilamination and distortion of the basement membranes (BMs) with an accumulation of laminin. Rupture of swollen epididymal ducts was observed, leading to an invasion of macrophages into the lumen. Male infertility was probably due to the combination of a developmental defect of the epididymis and the rupture of the epithelium resulting in the immotile spermatozoa. These results indicate that *Lgr4* has pivotal roles to play in the regulation of ESR1 expression, the control of duct elongation through BM remodeling, and the regional differentiation of the caput epididymidis.

developmental biology, epididymis, estradiol receptor, male reproductive tract, steroid hormone receptors

INTRODUCTION

Posttesticular sperm transit through the efferent ducts and epididymis in vivo is essential for sperm maturation, protection, and storage [1, 2]. The epididymis develops from the wolffian duct and is finally formed as a highly elongated and convoluted tubule that links the efferent ducts to the vas deferens. The adult epididymis anatomically consists of the caput, the corpus, and the cauda epididymidis. On the basis of macroscopic, histologic, ultrastructural, and histochemical observations, the caput epididymidis can be divided into five distinct regions [3]. Most proximal regions of the caput epididymidis, named the initial segment, consist of taller epithelial cells than any other caput regions. These regional differentiations, with the different cellular structures, are achieved within 28 days after birth [4]. Epididymal regions, having different morphologies and functions, show highly restricted gene expression patterns: for example, *Gpx5*, *Lcn2*, and *Etv4* are expressed in the whole caput epididymidis [5–7]. *Cst11*, *Cst12*, and *Lcn8* (previously known as *mEP17*) are expressed in the initial segment [6, 8]. The expressions of *Gpx5*, *Lcn2*, *Etv4*, and *Lcn8* are thought to be controlled by testicular fluid, which contains steroid hormones and growth factors such as fibroblast growth factors [5–7, 9, 10].

Steroid hormone receptors for androgen and estrogen are required for epididymal development and functioning. These roles were analyzed with mutant mice. The essential role of the androgen receptor (*Ar*), for early male development, was analyzed by examining the testicular feminization mutation (Ar^{Tfm}) in mice [11]. The Ar^{Tfm}/Y mice completely lack both the epididymis and the vas deferens. In addition to the *Ar*, two estrogen receptors (*Esr1* and *Esr2*) are expressed in the posttesticular tracts [12]. ESR1 (previously known as ERalpha) is mainly expressed in the efferent ducts; the $Esr1^{-/-}$ mice showed a water reabsorption failure in the efferent ducts and had a reduced male fertility rate [13, 14]. Recent reports indicate that ESR1 controls water reabsorption via regulation of *Slc9a3* (previously known as NHE3) and aquaporin 1 (*Aqp1*), which are both directly involved in the water reabsorption process [15]. In contrast to the $Esr1^{-/-}$ mice, the $Esr2^{-/-}$ mice did not show any abnormality in the development or function of either the efferent duct or the epididymis [16]. Production of double mutants of ESR1 and ESR2 confirms the pivotal role of ESR1, but not of ESR2, in the efferent ducts [17]. Although both of the estrogen receptors are expressed in the epididymis, their functions are not yet well understood.

Although it is clear that the AR is indispensable for the early development of the epididymis from the wolffian duct, other factors required for the development of the detailed regional compartmentalization are not well understood. When upper and middle wolffian duct epithelium is cultured on the seminal vesicle mesenchyme, this epithelium differentiates into the seminal vesicle epithelium [18]. This suggests that wolffian duct differentiation is controlled by the epithelial-mesenchymal interaction. Epithelial differentiation, induced by the mesen-

[1]Supported in part by KAKENHI (grant-in-aid for scientific research) in Priority Areas "Integrative Research Toward the Conquest of Cancer" from the Ministry of Education, Culture, Sports, Science, and Technology of Japan; a grant from the Osaka Foundation For the Promotion of Clinical Immunology; and a grant from the Pancreas Research Foundation of Japan.
[2]Correspondence: FAX: 81 96 373 6599;
e-mail: yamamura@gpo.kumamoto-u.ac.jp

Received: 11 June 2006.
First decision: 30 June 2006.
Accepted: 24 October 2006.

ISSN: 0006-3363. http://www.biolreprod.org

chyme, is well exemplified in ureteric bud branching of the developing kidneys. Since both kidneys and male reproductive tracts are developed from the same origin, the intermediate mesoderm, a similar set of signaling molecules may be involved in the development of both of these organs.

Possible factors accounting for this epithelial-mesenchymal interaction are bone morphogenetic protein (BMP) ligands and their related receptors. Disruption of *Bmp4*, *Bmp7*, *Bmp8a*, or *Bmp8b* shows that degeneration of the epididymal epithelium occurs in a region-specific manner [19–22]. $Bmp4^{+/-}$ mice especially showed epididymal degeneration in the corpus region. These results demonstrate that the BMP family ligands have a pivotal role in epididymal duct development and in maintaining its resulting integrity. Another possible factor that regulates the epithelial-mesenchymal interactions in the epididymis is ROS1, which is a member of the tyrosine kinase receptor family. In the developing kidneys, ROS1 is suggested as an upregulator of the expression of the extracellular matrix (ECM), which acts as a storage depot for various growth factors [23]. The $Ros1^{-/-}$ mice lack the initial segment [24]. These results suggest that detailed regional development is also dependent on highly regulated epithelial-mesenchymal interactions.

A recent study, by use of the $Lgr4^{-/-}$ mice obtained by the secretory trap approach, suggested an essential role for LGR4 in embryonic growth, especially for kidney and liver development [25]. In addition, $Lgr4^{-/-}$ mice with CD1 genetic backgrounds show the defective postnatal development of the epididymis [26]. This suggests that hypoplastic and dilated efferent ducts, as well as the epididymis, were all due to reduced cell proliferation rates and the blocking of the lumen by immune cell infiltrates, respectively. LGR family members are characterized by an extracellular domain with multiple leucine-rich repeats. The presence of a large extracellular domain is a remarkable feature that separates LGR family members from the other G protein-coupled receptors (GPCRs). Studies of LGRs from different species suggest that LGRs can be classified into three subtypes (A, B, and C) and that these three subtypes evolve during the early evolution of metazoans [27]. Type A LGRs include the FSH receptor, the LH receptor, and the thyroid-stimulating hormone receptor, in which the ligands are glycoprotein hormones. Type B LGR comprises three members: LGR4, also known as GPR48, LGR5, and LGR6. Type B LGR remains an orphan GPCR, and its physiological functions have not yet been determined. Type C LGRs, including LGR7 and LGR8, have recently been described as relaxin receptors. Following the identification of LGR7 and LGR8 as relaxin receptors, the closely related relaxin3 and INSL3 have been shown to function as selective agonists for LGR7 and LGR8, respectively.

We obtained an *Lgr4* hypomorphic mutant ($Lgr4^{Gt/Gt}$) with gene-trap insertional mutagenesis in embryonic stem cells with an exchangeable trap vector [28]. Contrary to the epididymides of the $Lgr4^{-/-}$ mice, by 8 wk after birth, the epididymides of *Lgr4* hypomorphic mutant mice have testicular fluid and contain immotile spermatozoa. Thus, we hypothesize that the epididymal phenotype of the $Lgr4^{Gt/Gt}$ male is unrelated to the transit blockage of the testicular fluid. Our mutant mice showed a milder phenotype than the null mutant mice in terms of their growth and perinatal death rate. Adult males of our mouse line showed short, dilated, and much less convoluted ducts in the epididymides. In the postnatal development of the epididymis, we found a reduction of ESR1 expression and a lack of an initial segment in the epididymides; furthermore, electron microscopic and immunohistochemical studies of the epididymal tubule structure in $Lgr4^{Gt/Gt}$ males indicated the disruption of the ECM structure with an increase of laminin. Our results suggest that the *Lgr4* gene regulates the postnatal epididymal morphogenesis via the maintenance of the ECM.

MATERIALS AND METHODS

Generation of Gene-Trap Mice

The Ayu21–127 embryonic stem clone was isolated in a gene-trap screening with the pU-21 vector. The pU-21 vector was generated by modifying the pU-17 vector [28]. This gene-trap mouse line was established by aggregating the embryonic stem cells with eight-cell embryos as described by Taniwaki et al. [28]. The chimeric male mice were crossed either with C57BL/6J or CBA/N Slc females. In this study, we used the F5 generation of mice. C57BL/6J mice were purchased from Charles River Japan Inc. (Yokohama, Japan). CBA/N Slc mice were purchased from Japan SLC Inc. (Hamamatsu, Japan). Mice were housed in the Center for Animal Resources and Development, Kumamoto University. All animal experiments were carried out with the approval of the Ethical Committee at the Center for Animal Resources and Development, Kumamoto University.

Cloning of Genomic DNA and Genotyping

Inverse PCR was performed to obtain flanking genomic DNA. DNA samples were isolated from the embryonic stem cells. After identification of the trap-vector insertion site, we set three PCR primers for genotyping. Genotyping was carried out by PCR with genomic DNA purified from a tail tip. To detect a wild-type allele, two primers were used: a 5′ primer, G1 (ACATCTACCCT-CTGCTTTCACC), and a 3′ primer, G2 (ATCCACTTGTTCCTGACCTGAG). G1 and another 3′ primer, G3 (AAGAACATAAAGTGACCCTCC), were used to detect a trapping allele. For PCR analysis, the DNA was subjected to 30 cycles (1 min at 94°C; 1 min at 62°C; and 1 min at 72°C) with 0.5 U of *Taq* polymerase (Perkin-Elmer, Foster City, CA).

Sperm Concentration and Motility Analysis

Sperm were collected from the cauda epididymidis at 8 wk of age and incubated in 200 μl of human tubal fluid (HTF) medium at 37°C for 1 h. The concentrations and motility rates were determined with a C-IMAGING C-MEN computerized semen analyzer (Compix Inc., Lake Oswego, OR). All counts were performed at 37°C. Motility was defined as linear direction at a speed of 50 μm/sec [29]. Viability of the incubated spermatozoa was assayed with the LIVE/DEAD Sperm Viability Kit (Invitrogen, Carlsbad, CA).

RNA Analysis

Rapid amplification of cDNA ends (RACE) by the 5′ RACE system (Invitrogen) was used to characterize the trapped gene. Total RNAs were extracted from various tissues and were used for RT-PCR and real-time PCR analyses. For Northern blot analysis, 1 mg of poly(A)+ RNAs isolated from various tissues was purified with the Oligotex-dT30 mRNA Purification Kit (Takara Shuzo, Kyoto, Japan). For the Northern blotting analysis, a murine *Lgr4* cDNA probe (probe A), a β-galactosidase probe (probe B), and a glyceraldehyde-3-phosphate dehydrogenase (*Gapdh*) probe were prepared with digitoxin (DIG)-labeled antisense riboprobes (Roche Molecular Biochemicals, Mannheim, Germany). Each cDNA template was amplified by RT-PCR, and the PCR product was then linked to a pGEM-T Easy Vector (Promega, Madison, WI). Transcription from the template vector was performed with SP6 or T7 on RNA polymerase and then purified on Quick Spin Columns (Bio-Rad, Hercules, CA). Primers used in the RT-PCR included the following: R1 (CTTCACCCAAGCACTGGATATCAG) located in the second exon; R2 (TGCAAAGCACTCAGTCCACGAATG) located in the third exon; and R3 (ACAGTATCGGCCTCAGGAAG) located in the splice acceptor of the trap vector. Real-time PCR was performed with SYBR Green (Takara Shuzo), and each RNA quantity was normalized to its respective *Gapdh* mRNA quantity.

Fertility Tests

$Lgr4^{Gt/Gt}$ mice 8–10 wk of age were used to mate with wild-type mice. +/*Gt* mice were also mated as a control. All mating completions were verified by examining vaginal plugs.

In Situ Hybridization

In situ hybridization analyses were performed on adult tissue sections with a VENTANA in situ hybridization machine (Ventana Medical Systems Inc., Tucson, AZ). All tissues were fixed with 4% paraformaldehyde in PBS for 48 h at

room temperature and cryosectioned. The DIG-labeled *Gpx5*, *Lcn2*, *Cst12*, and *Lcn8* antisense and sense riboprobes (Roche) were prepared as described above.

Measurement of Serum Estradiol and Testosterone

Serum estradiol and testosterone concentrations were measured commercially by RIA (SRL Inc., Tokyo, Japan) when the mice were 8 wk of age. To measure the serum estradiol and testosterone levels, blood was withdrawn from the retro-orbital sinus by penetrating the retro-orbital sinus/plexus with a glass capillary tube after the mice were anesthetized with ether.

Detection of β-galactosidase Activities

To detect LGR4 expression levels, we determined the β-galactosidase activity produced by the trapped allele. Samples were fixed for 30–60 min at room temperature in 1% formaldehyde, 0.2% glutaraldehyde, and 0.02% NP-40. Fixed samples were washed two times in PBS and incubated for 16 h at 37°C in a staining solution of 5 mM potassium ferricyanide, 5 mM potassium ferrocyanide, 2 mM $MgCl_2$, and 0.5% X-gal in PBS. Samples were washed twice in PBS and then postfixed in 4% paraformaldehyde.

Immunohistochemical Staining

Epididymal tissues were fixed with 4% paraformaldehyde in PBS for 24 h at 4°C. Paraffin-embedded tissues were sectioned, dewaxed, and rehydrated. Frozen sections were used to determine type IV collagen and laminin expression levels. Sections were incubated with the primary antibody in 3% BSA in PBS for 16 h at 4°C. In the present study, the following antibodies and dilutions were used: diluted anti-ESR1 (DAKO, Carpinteria, CA), 1:2; anti-ESR2 (Chemicon, Temecula, CA), 1:500; anti-AR (Santa Cruz Biotechnology, Inc., Santa Cruz, CA), 1:500; anti-type IV collagen (Southern Biotech, Birmingham, AL), 1:8000; anti-laminin (DAKO), 1:6000; anti-CD68 (Serotec), 1:100; and anti-MSR1 (unpublished results). After washing, sections were incubated with the corresponding secondary antibodies (all in 1:200 dilutions) for 1 h at room temperature. To detect with anti-mouse antibody, sections were blocked with a commercially available reagent and detected with a commercial kit (Vector Laboratories, Burlingame, CA). The Vectastain ABC Kit (Vector Laboratories) was used for the avidin-biotin complex method according to the manufacturer's instructions and detected with diaminobenzidine. Immunofluorescent signals were observed with a TCS-SP2 AOBS confocal microscope (Leica Microsystems).

Western Blot Analysis

The epididymides were homogenized in a lysate buffer and purified with acetone precipitation. Extracts were applied to 8% polyacrylamide gel electrophoresis and transferred to an Immobilon polyvinylidene difluoride filter (Millipore, Billerica, MA). Primary antibodies for the following antigens were used at the indicated dilutions: anti-type IV collagen (LSL, Tokyo, Japan), 1:500; anti-laminin (DAKO), 1:500; anti-AR (Santa Cruz Biotechnology), 1:500; and anti-actin (Santa Cruz Biotechnology), 1:500. Anti-rabbit (Amersham Biosciences) or anti-goat (Santa Cruz Biotechnology) immunoglobulin G antibody conjugated with horseradish peroxidase was used for detection purposes.

Electron Microscopy

Spermatozoa collected from cauda epididymidis were incubated in HTF medium for 30 min and fixed in HTF medium with 2% glutaraldehyde for 20 min. The samples were postfixed in an unbuffered 2% osmium tetroxide solution for 3 h and then dehydrated in ascending grades of alcohol. Subsequently, they were critically point dried, osmium plasma coated, and examined by a Jeol JSM 6320 F scanning electron microscope (Jeol Ltd., Tokyo, Japan). The caput epididymides in 5-wk-old males were fixed with 2.5% glutaraldehyde and postfixed with 1% osmium tetroxide. After dehydration in a graded series of ethanol and propylene oxide, the samples were embedded in epoxy resin. Ultrathin sections were stained with uranyl acetate and lead citrate and then imaged with an H-7500 electron microscope (Hitachi, Tokyo, Japan).

RESULTS

Establishment of Ayu21–127 Line and Identification of Trapped Genes

We performed gene-trap mutagenesis in embryonic stem cells with pU-21 trap vectors (Fig. 1A) and thereby isolated 88

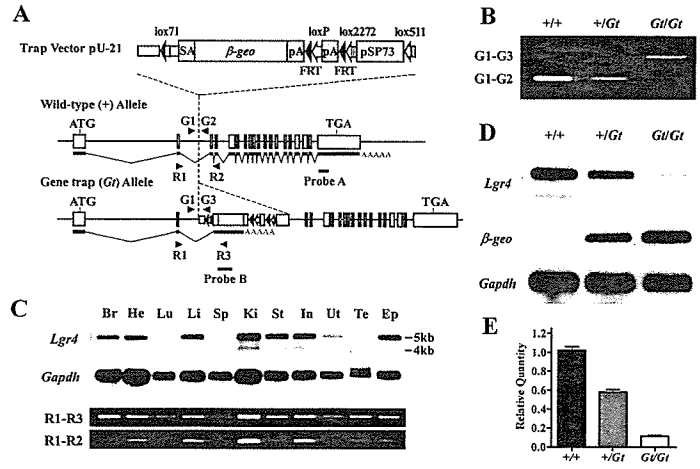

FIG. 1. Hypomorphic mutant of the *Lgr4* gene. **A**) The trap vector, pU-21, was inserted into the second intron of the *Lgr4* gene. G1–3 primers (red arrowheads) were used for the genotyping, and R1–3 primers (blue arrowheads) were used for RT-PCR to detect endogenous *Lgr4* mRNA or fusion mRNA. DIG-labeled RNA probes (probes A and B) were used for the Northern blot analysis. **B**) PCR genotyping. The wild-type (+) or trap (*Gt*) allele is detected with G1 and G2 or G1 and G3 primer sets, respectively. **C**) Northern blotting analyses (upper) and RT-PCR analyses (lower) with various tissues +/+ and *Gt*/+ mice, respectively. Br, Brain; He, heart; Lu, lung; Li, liver; Sp, spleen; Ki, kidneys; St, stomach; In, intestine; Ut, uterus; Te, testes; Ep, epididymides. **D**) Northern blot analyses with kidney extracts to detect *Lgr4* and fusion mRNA in each genotype. **E**) Quantitative RT-PCR analysis with newborn brain extracts to detect *Lgr4* mRNA in each genotype.

gene-trap embryonic stem clones. We identified trapped genes by the 5′ RACE. Several mutant mouse lines were established through the production of chimeric mice with these trapped embryonic stem clones. Among these lines, we selected the 127 line, termed the B6;CB-$Lgr4^{GtAyu21\text{-}127Imeg}$ ($Lgr4^{Gt}$) in which the *Lgr4* is trapped, to further analyze the physiological functions of LGR4. Southern blot analysis, with a vector fragment as a probe, indicated a single-copy integration of the vector (data not shown). Analysis of the genomic region around the insertion site revealed that the trap vector was integrated into the second intron of the *Lgr4* gene (Fig. 1A). We confirmed that the trap-vector integration event resulted in either a 628- or 562-bp deletion in the 5′ or 3′ region of the trap vector, respectively. No deletion occurred in the genomic region around the insertion site. Genotyping was done with G1 and G2 primers for a wild-type (+) allele and G1 and G3 primers for the gene-trap (*Gt*) allele (Fig. 1B).

Northern blot analysis, with various adult tissues of wild-type mice, indicated the broad expression of the *Lgr4* gene as described by Mazerbourg et al. [25] and Schoore et al. [30]. RT-PCR analyses, with tissues of $Lgr4^{+/Gt}$ mice the same as in Northern blot analyses, showed that all tissues had the fusion mRNA composed of exons 1 and 2 in the *Lgr4* gene and of a β-*geo* gene of the trap vector (Fig. 1C). Mating between $Lgr4^{+/Gt}$ parents generated $Lgr4^{Gt/Gt}$ mice. Northern blot analysis and quantitative RT-PCR showed that the $Lgr4^{Gt/Gt}$ mice had 10% mRNA expression of the *Lgr4* gene (Fig. 1, D and E). These results prove that the $Lgr4^{Gt/Gt}$ mouse is a hypomorphic mutant.

Growth Retardation

We investigated the ratio of each genotype among the newborn mice obtained by the mating of the $Lgr4^{+/Gt}$ parents, and the resulting ratio was consistent with the expected

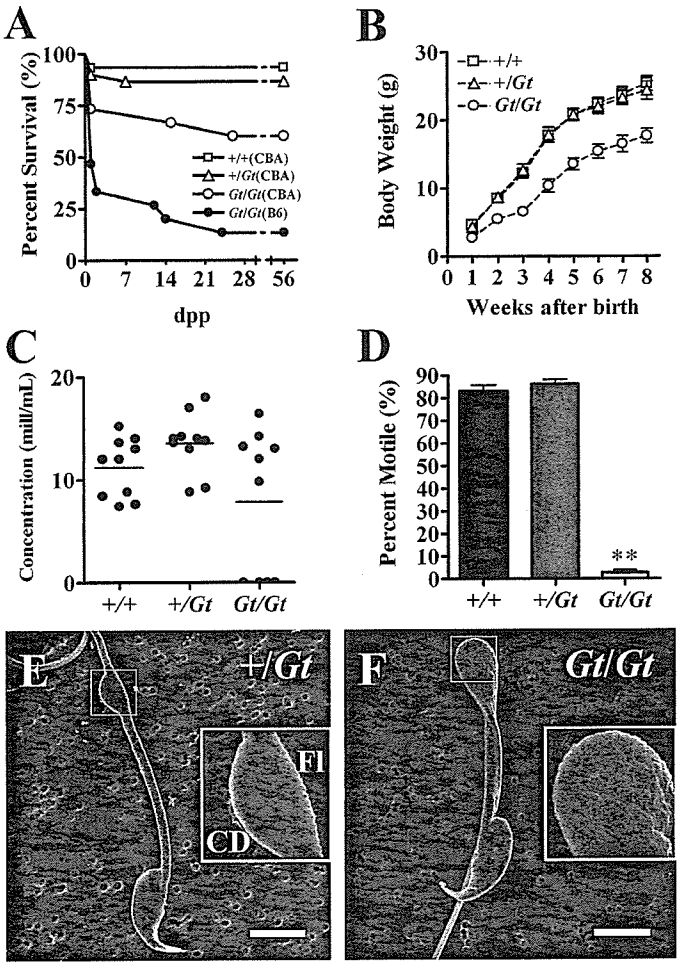

FIG. 2. *Lgr4*$^{Gt/Gt}$ mice showed a male-sterile phenotype. **A**) Survival rate of each genotype. Homozygotes are measured on the CBA and C57BL/6J (B6) genetic background (n = 15). **B**) Growth curve of the +/+, +/*Gt*, and *Gt*/*Gt* mice from birth to adulthood (n = 10; mean ± SEM). **C**) Caudal sperm concentrations at 8 wk of age in each genotype. The sperm concentration in 200 μl of HTF medium, prepared in the same way as for the sperm for performing in vitro fertilization, was measured (n = 10; bar = mean). **D**) Percent motile of caudal sperm at 8 wk of age in each genotype. $^{**}P < 0.01$ (unpaired Student *t*-test) vs. +/+ males; n = 10 in +/+ and +/*Gt*, n = 6 in *Gt*/*Gt*; mean ± SEM. **E, F**) Scanning electron microscope of the spermatozoa of +/+ and *Gt*/*Gt* males. Each inset indicates the higher magnification of cytoplasmic droplet (CD) and flagellum (Fl) at the midpiece-principal piece junction on the spermatozoa. Bar = 5 μm (**E, F**).

mendelian distribution. With the C57BL/6J genetic background, about 85% of the homozygous mice died during the postnatal development period (Fig. 2A); however, with the CBA genetic background, 60% of the offspring survived, but they showed growth retardation (Fig. 2, A and B). Offspring in the CBA background group were used in the following studies.

Male Infertility

To analyze fertility, we carried out a breeding test (Table 1). *Lgr4*$^{Gt/Gt}$ males exhibited normal copulative behaviors. Although we confirmed that the vaginal plug in all wild-type females mated with *Lgr4*$^{Gt/Gt}$ males, no pregnancies were observed. Although the pregnancy rate between wild-type males and *Lgr4*$^{Gt/Gt}$ females was reduced, the impregnated females sired and nursed their pups normally. These results indicate that the *Lgr4* deficiency causes infertility in the male but not in the female.

TABLE 1. Fertility tests of *Lgr4*$^{Gt/Gt}$ mice.

Cross					Genotyping of offspring	
Male	Female	Matings	Births	No. of offspring	+/+	+/*Gt*
Gt/*Gt*	+/+	7	0	0	0	0
+/*Gt*	+/+	4	4	33	17	16
+/+	+/*Gt*	4	4	28	15	13
+/+	*Gt*/*Gt*	7	5	23	0	23

Immotile Sperm

To examine the reason for the male infertility, we first analyzed sperm concentrations and motility in the cauda epididymidis of *Lgr4*$^{Gt/Gt}$ males. The concentration of spermatozoa in the cauda epididymidis of *Lgr4*$^{Gt/Gt}$ males was very variable, but there were no intragroup differences in sperm concentrations (Fig. 2C). However, almost all of the spermatozoa in the homozygous epididymides were either immotile or much less motile than normal (Fig. 2D). Sperm viability assay, by means of staining with SYBR14 and propidium iodide, demonstrated that the mean ± SD of live/dead spermatozoa in three individuals were 252.3 ± 67.0/147.0 ± 30.3 and 1.7 ± 1.5/317.0 ± 121.2 in +/*Gt* and *Gt*/*Gt*, respectively, indicating that the viability was significantly decreased in *Lgr4*$^{Gt/Gt}$ males. Electron microscopic studies showed a hairpin structure of spermatozoa at the midpiece-principal piece junction and large cytoplasmic droplet (Fig. 2, E and F). The boundary between sperm flagellum and cytoplasmic droplet was obscure (Fig. 2F). These data suggested that the male infertility of *Lgr4*$^{Gt/Gt}$ mice was caused by the immotility and abnormal structure of the sperm.

Rete Testis Dilation and ESR1 Reduction in Efferent Ducts

To examine the effect on spermatogenesis, we analyzed the testes. There were no significant differences in testis weight between wild types, heterozygotes, and homozygotes 8 wk of age; however, as shown in Figure 3A, there was a tendency of testis weight in homozygous mice to be slightly increased over that of the wild-type or heterozygous mice. Histologic analysis of the testes in *Lgr4*$^{Gt/Gt}$ males revealed rete testis dilation, luminal swelling, and atrophy of the germinal epithelium of the seminiferous tubules (Fig. 3, B and C). Rete testis dilation was previously reported in *Esr1*$^{-/-}$ or *Slc9a3*$^{-/-}$ mice [14, 15]. Furthermore, ESR1 and SLC9A3 are both now well-known key molecules that regulate water reabsorption in efferent ducts [13]. To examine the expression levels of ESR1 and SLC9A3, we performed immunohistochemical analyses with anti-ESR1 and anti-SLC9A3 antibodies. At 8 wk of age, both molecules were detected in the epithelial cells of the efferent ducts of the wild-type mice (Fig. 3, D and E). On the other hand, the levels of ESR1 and SLC9A3 expression in the efferent ducts of *Lgr4*$^{Gt/Gt}$ males 8 wk of age were lower than those in the wild-type males (Fig. 3, F and G).

Taken together, these results suggest that ESR1 reduction results in a water reabsorption failure, which leads to rete testis dilation and spermatogenesis impairment in *Lgr4*$^{Gt/Gt}$ males.

Developmental Defect in the Epididymis of Lgr4$^{Gt/Gt}$ *Males*

Weight of the epididymides in *Lgr4*$^{Gt/Gt}$ males was significantly lower than that of wild-type and heterozygous littermates (Fig. 3A). Macroscopically, the epididymides contained short and dilated tubules with uneven sperm distribution (Fig. 4A). As ESR1 and SLC9A3 expression was

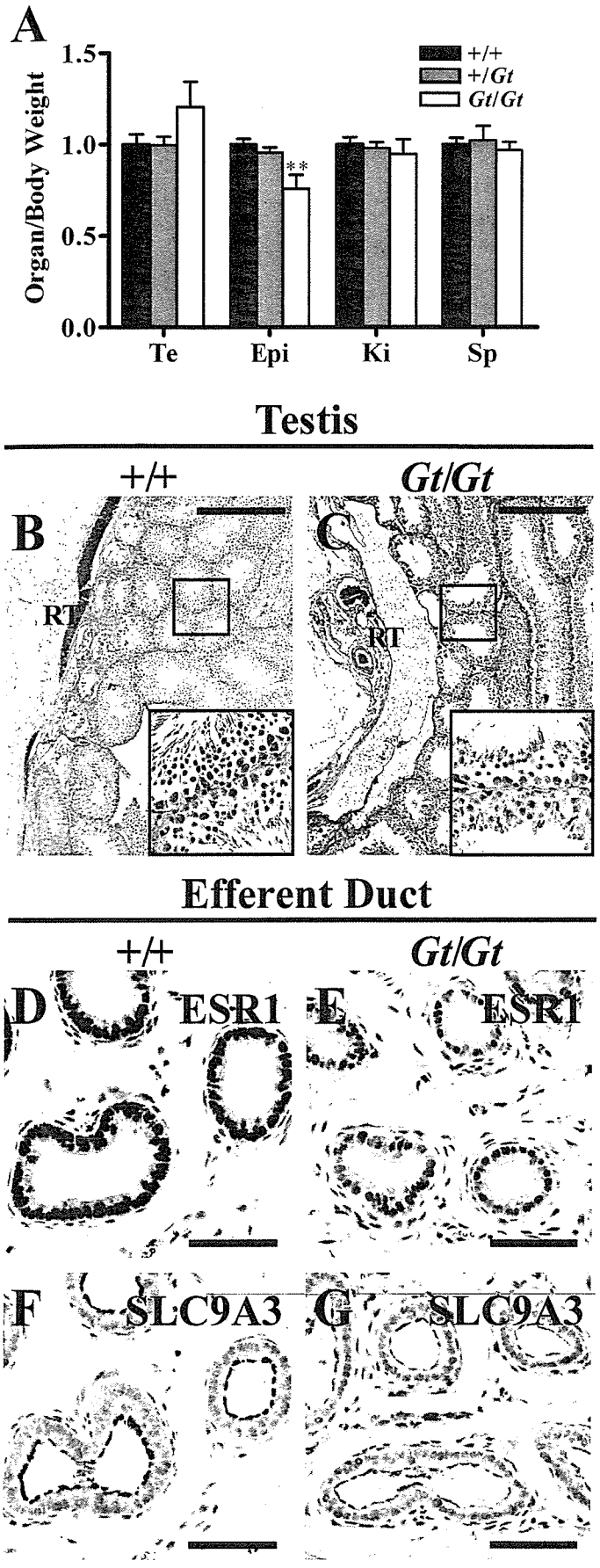

FIG. 3. Rete testis dilation and ESR1 reduction in the efferent ducts. **A**) Relative reproductive organ weight in each genotype. $^{**}P < 0.01$ (unpaired Student *t*-test) vs. +/+ males; n = 8; mean ± SEM. Te, Testes; Ep, epididymides; Ki, kidneys; Sp, spleen. **B**, **C**) Testis histology of 8-wk-old males in +/+ and *Gt/Gt* males. Each inset indicates the higher magnification of the seminiferous tubules. Immunostaining for ESR1 (**D**, **E**) and SLC9A3 (**F**, **G**) in the efferent ducts of 8-wk-old males in +/+ and *Gt/Gt* males. Bar = 400 μm (**B**, **C**) and 50 μm (**D**–**G**).

reduced in the efferent ducts, we also examined the expression of ESR1 and SLC9A3 in the epididymis. In the epithelial cells of the caput epididymidis, only ESR1 was detectable (Fig. 4, B and C). The expression level of ESR1 in $Lgr4^{Gt/Gt}$ males was much lower than in wild-type males (Fig. 4D). SLC9A3 staining was not detectable in the caput epididymidis of $Lgr4^{Gt/Gt}$ males (Fig. 4E). We further examined when the expression of ESR1 started to decrease during the postnatal epididymal development in $Lgr4^{Gt/Gt}$ males. The ESR1 expression level increased gradually up to 3 wk of age in the caput epididymidis of the control littermates (Fig. 4, F–I). In contrast, the ESR1 expression level decreased and disappeared by 3 wk of age in $Lgr4^{Gt/Gt}$ males (Fig. 4, J–M).

Contrary to the sharp decrease of ESR1 expression level, the expression of AR and ESR2 was normal during the development of the epididymides (Fig. 4, N–Q). In addition, we measured the serum estradiol and testosterone levels in 8-wk-old mice; however, there were no significant differences in serum estrogen or testosterone levels between wild-type and $Lgr4^{Gt/Gt}$ mice (Fig. 4, R and S).

By 35 days after birth, the normal mature caput epididymidis can be subdivided into three regions: initial segment, proximal caput, and distal caput [31]. The initial segment in the epididymis of wild-type males is distinct from the other caput regions. To examine the differentiation of the epididymal region in $Lgr4^{Gt/Gt}$ males, we performed a section in situ hybridization with antisense riboprobes for marker mRNAs, *Cst12* [8], and *Lcn8*, also known as *mEP17* [6, 32], *Gpx5* [7], and *Lcn2* [6]. *Cst12* and *Lcn8* were shown to be expressed in the initial segments that differentiated first in the whole caput epididymidis. We could detect the expression of *Cst12* and *Lcn8* in wild-type mice (Fig. 5, A and C) but not in $Lgr4^{Gt/Gt}$ mice (Fig. 5, B and D). On the other hand, *Gpx5* and *Lcn2* were shown to be expressed in the proximal epididymis region. We detected the strong expression of *Gpx5* and *Lcn2* in the proximal epididymis regions in both wild-type and $Lgr4^{Gt/Gt}$ mice (Fig. 5, E–H). These results suggest that LGR4 has an essential role in the differentiation of the initial segment during the postnatal development period of the epididymis.

Electron Microscopic Analysis of Caput Epididymal Tubules

To determine the cause for the epididymal abnormal morphogenesis in $Lgr4^{Gt/Gt}$ males, we performed transmission electron microscopic analysis at 5 wk after birth. In wild-type males, epithelial cells in the caput epididymal tubules displayed numerous vesicles and coated pits indicative of active endocytosis, and they also displayed an expanded Golgi apparatus at the upper side of the nucleus (Fig. 6A). In $Lgr4^{Gt/Gt}$ males, epithelial cells showed less endocytosis and few secretion components (Fig. 6B). We also observed detachment of basal cells from adjacent epithelial cells in $Lgr4^{Gt/Gt}$ males (Fig. 6B). In some epithelial layers, we found macrophage-like cells, which have amoebic cell membranes and lysosomal granules, on the basal side (Fig. 6C), but not on the apical side, of the epithelial cell layer.

Normally, these epithelial cells form the blood-epididymal barrier (BEB), which regulates small substance transition into the lumen of the epididymal tubules and protects spermatozoa

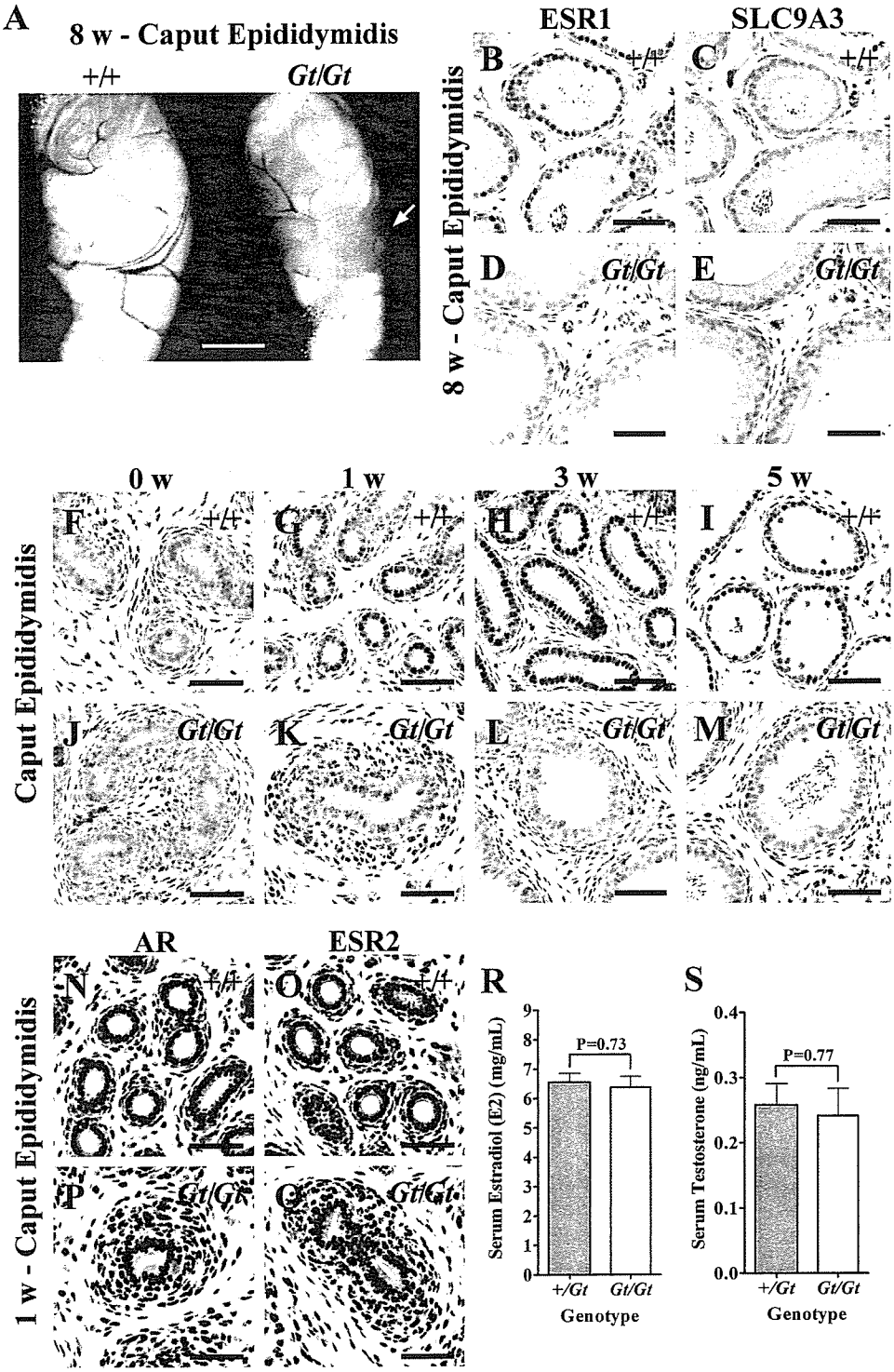

FIG. 4. Decreased expression of ESR1 in mutant caput epididymidis. **A**) Morphology of the caput epididymidis of the +/+ and *Gt/Gt* males. White arrow indicates the clear region that lacks sperm in the tubule. **B–E**) Immunostaining for ESR1 and SLC9A3 in the caput epididymides of 8-wk-old males. **F–M**) Immunostaining for ESR1 in the caput epididymidis of +/+ and *Gt/Gt* males 0, 1, 3, and 5 wk of age. **N–Q**) Immunostaining for AR and ESR2 in the caput epididymidis of +/+ and *Gt/Gt* males 1 wk of age. **R, S**) Serum estradiol and testosterone levels of +/*Gt* and *Gt/Gt* males 8 wk of age. Bar = 1 mm (**A**) and 50 μm (**B–Q**).

from attack by the self immune system, like the blood-brain barrier, blood-thymus barrier, and blood-testis barrier [33]. In the epididymis, formation of the BEB is accomplished by the tight junction between the apical sides of the epithelial cells [33]. Thus, we examined the tight junction formation at a higher magnification; however, we did not observe any abnormalities in the tight junctions (Fig. 6, D–F).

The basement membranes (BMs) of wild types appeared as a thin continuous layer closely in contact with basal cells, which usually form a monolayer (Fig. 6G). In $Lgr4^{Gt/Gt}$ males, the BMs showed multilamination and distortion (Fig. 6, H and I). In addition, an accumulation of ECM-like material was observed toward the mesenchymal cell layers (Fig. 6, H and I).

Laminin Accumulation in the Epididymis

To characterize the ECM-like deposits in the BM in detail, we performed periodic acid-methenamine-silver (PAM) staining. In the caput epididymidis of $Lgr4^{Gt/Gt}$ mice, the distribution of the ECM, as demonstrated by PAM staining, was more diffuse around the mesenchymal cell layer than it was in wild-type mice (Fig. 7, A–D). In the epididymis, the ECM is composed primarily of type IV collagen and laminin

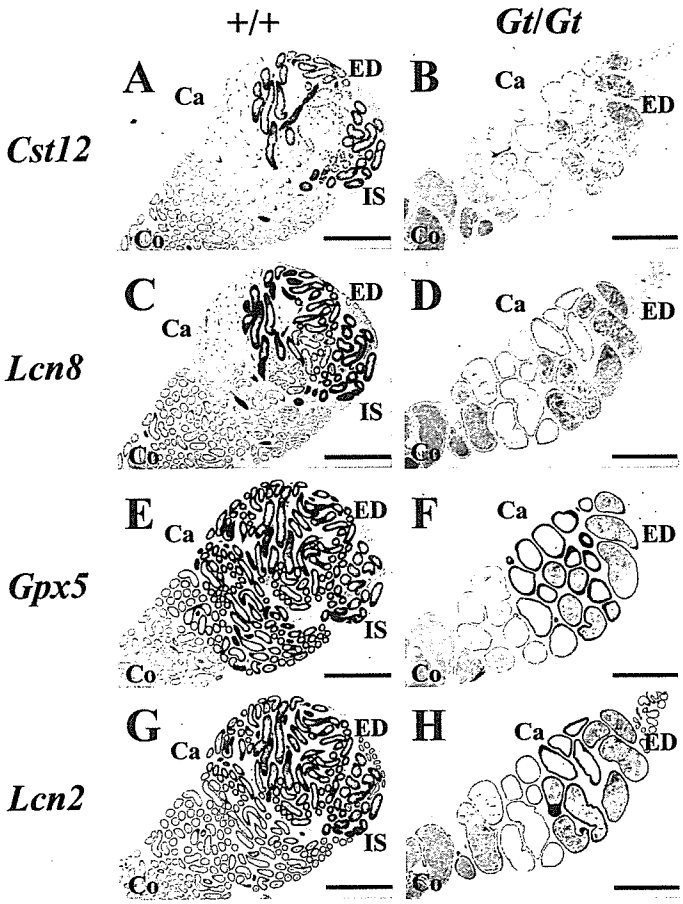

FIG. 5. Section in situ hybridization of *Cst12* (**A**, **B**), *Lcn8* (**C**, **D**), *Gpx5* (**E**, **F**), and *Lcn2* (**G**, **H**) in the efferent ducts (ED), caput (Ca), and proximal corpus (Co) epididymidis of +/+ (**A**, **C**, **E**, **G**) and *Gt/Gt* males (**B**, **D**, **F**, **H**) 8 wk of age. *Cst12* and *Lcn8* signals indicate the initial segment (IS) in the caput epididymidis. Bar = 1.0 mm.

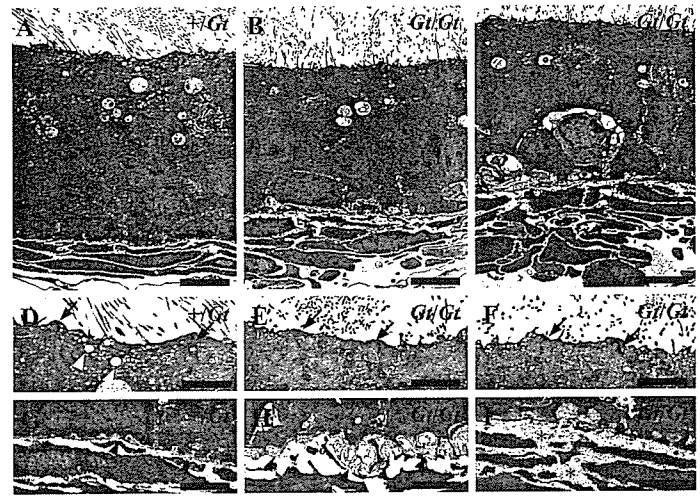

FIG. 6. Electron microscopy of the caput epididymidis of *+/Gt* and *Gt/Gt* males 5 wk of age. **A**) Normal epithelial and peripheral cell layers of the caput epididymal tubules in *+/Gt* males. **B**) Detachment of basal cells and thickening of the peripheral cell layer of the caput epididymal tubules in *Gt/Gt* males. **C**) Macrophage-like cell invasion into the epithelial cell layer in *Gt/Gt* males. **D–F**) Apical surface of the epithelial cells. Smooth surfaced secretory vesicles (open arrowheads) and small vesicles in *+/Gt* males are not seen in *Gt/Gt* males. Tight junctions (black arrows) at the apical surface between epithelial cells were observed in both genotypes. **G–I**) Basement membranes under the epithelial cell layers (black arrowheads). A consecutive thin layer was observed in *+/Gt* males. In *Gt/Gt* males, basement membranes with multilayers (**H**) or depositions (**I**) were observed. Bar = 5 μm (**A–C**) and 2.5 μm (**D–I**).

isoforms [34]. Immunohistochemical analysis for type IV collagen showed similar staining in the caput and cauda of both wild-type and $Lgr4^{Gt/Gt}$ mice (Fig. 7, E–H). On the other hand, immunohistochemical analysis for laminin showed intense staining in the caput epididymidis (Fig. 7, I and J) but not in the cauda epididymidis (Fig. 7, K and L) of $Lgr4^{Gt/Gt}$ mice. Laminin positive staining was observed, though in the lumen of the cauda epididymidis (Fig. 7L). As expected, the total amount of laminin in the epididymides was increased in $Lgr4^{Gt/Gt}$ males, as was verified by Western blot analysis (Fig. 7M). Double staining with DAPI (4′,6′-diamidino-2-phenylindole), which can stain spermatozoal nuclei, and anti-laminin antibody indicated that the laminin bound to the sperm heads of $Lgr4^{Gt/Gt}$ males (Fig. 7, N–S). These results suggest that laminin accumulation in the BM contributes to the abnormal morphology of the epididymis and that the laminin is somehow leaked into the lumen.

Macrophages in the Lumen of the Epididymal Tubules

With electron microscopic analysis, we discovered macrophage-like cells in the epithelium. These macrophage-like cells were observed under the tight junctions of the epithelial cells. To confirm whether these cells were macrophages, we performed immunohistochemical staining for CD68 and MSR1 (known as CD204). In the wild-type mice, CD68, but not MSR1, was detected in the epithelial cells of segment III of the caput epididymidis; both of these molecules are well-known macrophage markers (Fig. 8, A and B). The CD68 staining, at the differentiated epididymal region, was not observed in the epithelium of the $Lgr4^{Gt/Gt}$ epididymides. This result was consistent with the previous result that an initial segment was missing in $Lgr4^{Gt/Gt}$ males. This was detected by a section in situ hybridization with the *Cst12* and *Lcn8* as probes. In the wild-type mice, except for segment III of the caput epididymidis, CD68 or MSR1 positive cells were seen only in the interstitial tissues of the caput epididymidis; they were not seen in either the lumen or epithelium (Fig. 8, C and D). On the other hand, CD68 and/or MSR1 positive cells were sparsely distributed in some areas of both the lumen and the epithelium of the $Lgr4^{Gt/Gt}$ epididymides (Fig. 8, E–H). All the positive macrophage marker cells between the epithelial cells were seen under the apical surface of the epithelial cell layer (Fig. 8, G and H). In a few $Lgr4^{Gt/Gt}$ males, we did not observe any macrophages in the lumen (Fig. 8, I and J). Massive macrophage intrusions were seen near the ruptured tubule structures (Fig. 8, K and L). These results suggest that dilation of the tubules, caused by water retention, disrupts the tubular structure, thereby leading to an intrusion of macrophages into the lumen.

LGR4 Expression in the Epididymis

As described previously, the integration of trap vectors resulted in the production of fusion mRNA encoding marker genes, β-*geo*, which expression is directed by the *Lgr4* endogenous promoter. Thus, we expect that the expression of the markers in heterozygotes is a reflection of LGR4 expression. We also analyzed the expression pattern of β-*geo* in heterozygous mice. X-gal staining of fetal male reproductive tracts demonstrated that *Lgr4* expression begins at 17.5 days postconception in the wolffian duct from the proximal region

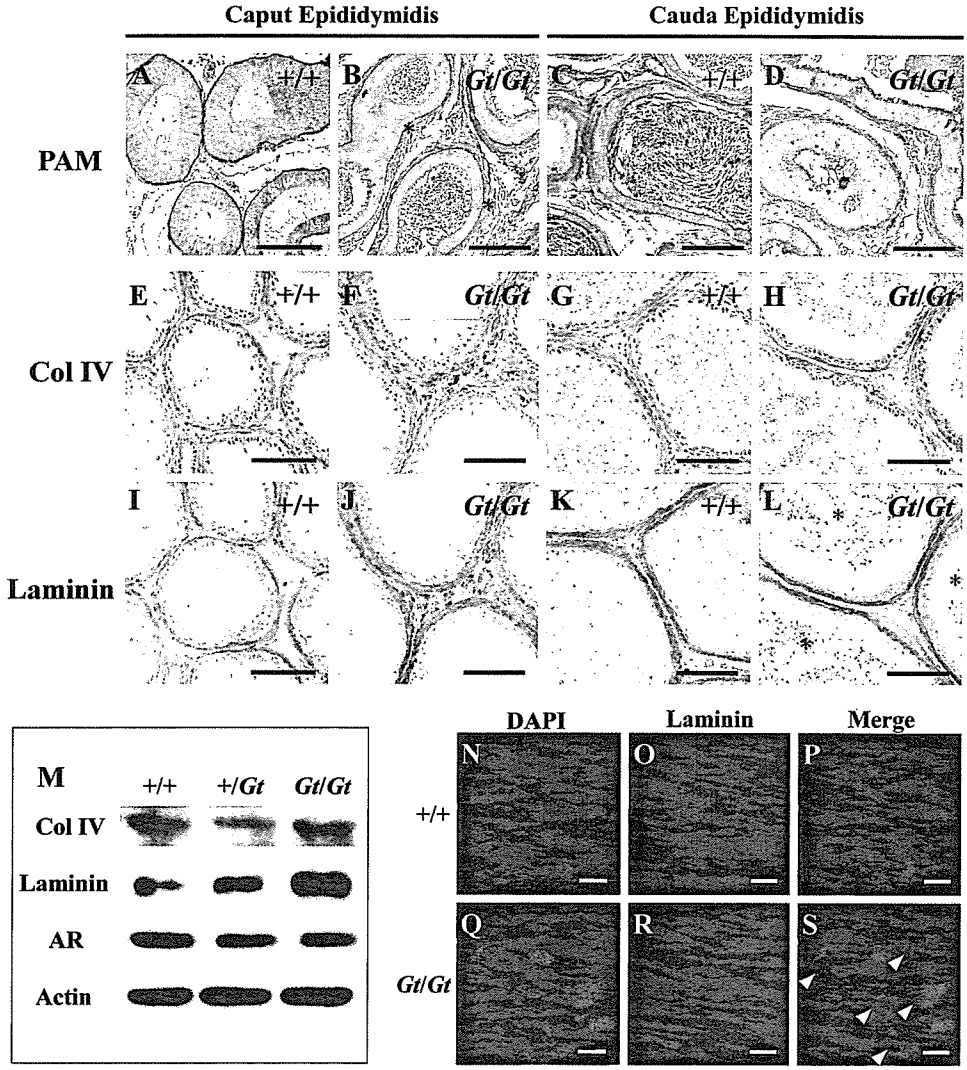

FIG. 7. Alteration of ECM components in the epididymides of *Gt/Gt* males 8 wk of age. PAM staining (**A–D**) and immunostaining for type IV collagen (**E–H**) and laminin (**I–L**). Strong signals of laminin were detected at the caput epididymal tubules (black arrows in **J**) and at the lumen of the cauda epididymal tubules (asterisk in **L**). **M**) Western blotting analyses for type IV collagen (Col IV), laminin, AR, and actin. Polyclonal laminin antibody, which is used in immunohistochemistry, detected the 250-kDa laminin components as a single positive band. AR and actin were used as controls. **N–S**) Immunofluorescence staining for laminin with the spermatozoa in the cauda epididymidis of +/+ and *Gt/Gt* males. Bar = 100 μm (**A–L**) and 5μm (**N–S**).

(data not shown). The initiation of *Lgr4* expression precedes the initiation of extensive elongation and convolution of the epididymal tubules, which occurs during the first days after birth. We also observed that *Lgr4* expression was detected in the ovaries at 17.5 days postconception (data not shown). Although Mazerbourg et al. [25] described infertility in females, our homozygous females were fertile (Table 1). One-tenth the normal expression level of *Lgr4* may be sufficient to overcome the phenotype in females. At the newborn stage, β-*geo* expression was higher in the testes than in the epididymides (Fig. 9A). At 1 wk of age, though, β-*geo* expression level in the epididymides became similar to that in the testes (Fig. 9B). Strong signals were detected in the mesenchymal cells located directly below the epithelium of both the efferent ducts and caput epididymidis (Fig. 9, C–J).

DISCUSSION

In this study, we demonstrated a role for *Lgr4* in the development of the epididymis with the *Lgr4* hypomorphic mutant mice generated by gene-trap insertional mutagenesis.

Mazerbourg et al. [25] reported that $Lgr4^{-/-}$ mice exhibited intrauterine growth retardation associated with embryonic and perinatal lethality in the C57BL/6 background, thus preventing analysis of either the postnatal or adult phenotype. Recently, Mendive et al. [26] showed that the same $Lgr4^{-/-}$ mice with the CD1 genetic background were viable and that most of them reached adulthood. They also demonstrated defective postnatal development of the male reproductive tract. We found that the $Lgr4^{-/-}$ and $Lgr4^{Gt/Gt}$ mice have overlapping phenotypes, as described by Mendive et al. There are, however, distinct differences between their $Lgr4^{-/-}$ and our $Lgr4^{Gt/Gt}$ mice.

First, our mutant mice line has 10% of the normal transcripts, suggesting that these 10% of transcripts skipped the splice acceptor in the trap vector. This residual activity may be the reason for the 15% survival rate to adulthood of $Lgr4^{Gt/Gt}$ mice with the C57BL/6 background. With this hypomorphic mutant line, we were able to reveal the hidden phenotypes that do not appear in the null mutant. Null mutant mice, which are embryonic lethal, sometimes become viable by changing their genetic background, thus making it possible to analyze these phenotypes in the adult stage. However, the phenotypes observed in these mutants might be a reflection of a modifier gene. On the other hand, we can analyze the phenotypes that are directly caused by the low level expression of *Lgr4*.

In the testes, luminal swelling, loss of germinal epithelium of the seminiferous tubules, and rete testis dilation were observed. The same phenotypes were also observed in $Lgr4^{-/-}$ mice. One reason for this is the decreased expression levels of ESR1 and SLC9A3 in the efferent ducts (Fig. 3, F and G), as both ESR1 and SLC9A3 are well-known key water reabsorption-regulating molecules in the efferent ducts [13]. In fact, similar phenotypes were observed in $Esr1^{-/-}$ mice [14] and

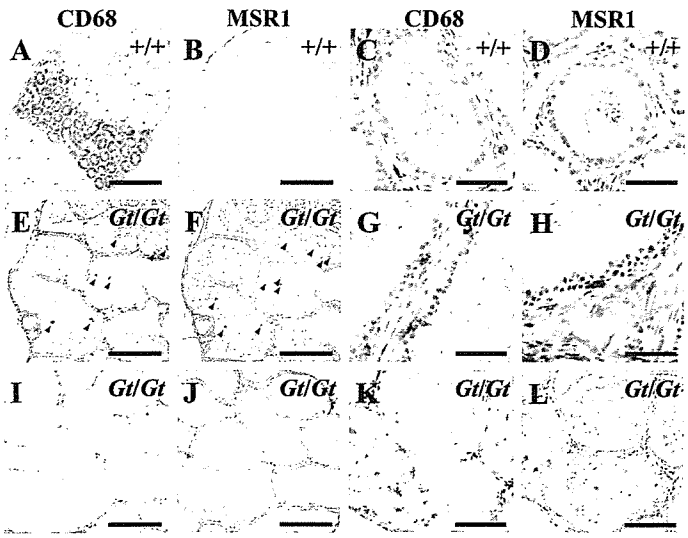

FIG. 8. Immunostaining for CD68 (**A–C** and **G–I**) and MSR1 (**D–F**, **J–L**) in the caput (**A–H**, **J**, **K**) and the corpus (**I**, **L**) epididymidis. **A**) In the control, CD68 was positive in the epithelial cells at segment III of the caput epididymidis. **A–D**) Both CD68 and MSR1 were positive in some interstitial cells. **E**, **F**) In *Gt/Gt* males, CD68 and MSR1 positive signals showed macrophages in the lumens of the caput epididymal tubules. **G**, **H**) Most CD68 and MSR1 positive cells were detected in the interstitial tissues and basal sides of the epithelial cell layers. **I**, **J**) Contrary to **E** and **F**, some of the caput epididymides of the *Gt/Gt* males were negative. **K**, **L**) CD68 and MSR1 positive cells in the lumens of the epididymal tubules. Injured tubules were detected near a swarm of macrophages. Bar = 500 μm (**A**, **B**, **E**, **F**, **I**, **J**), 50 μm (**C**, **D**, **G**, **H**), and 200 μm (**K**, **L**).

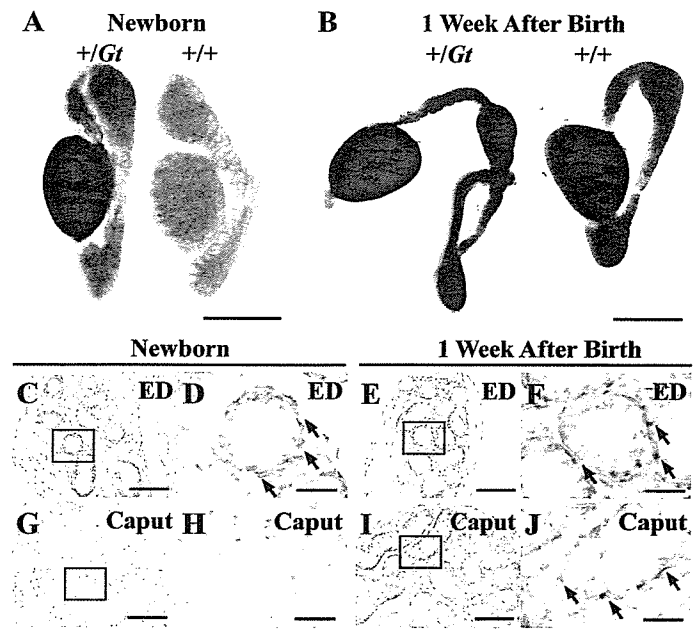

FIG. 9. *Lgr4* expressions levels in the male reproductive tracts. *Lgr4* expression levels are detected in the epididymides from the perinatal stage, and most of them have been localized at the peritubular cells. Whole-mount X-gal staining of the testes, efferent ducts (ED), and epididymides in newborns (**A**) and 1 wk after birth (**B**). Sections of the X-gal-stained efferent ducts (**C–F**) and epididymides (**G–J**) of *+/Gt* males in newborns (**C–E**, **H**) and 1 wk after birth (**E**, **F**, **I**, **J**), respectively. **D**, **F**, **H**, **J**) Higher magnification of the area indicated by the boxes in **C**, **E**, **G**, and **I**, respectively. Arrows in **D**, **F**, and **J** indicate strong signals at the peritubular cells located directly below the epithelium. Bar = 1 mm (**A**, **B**), 100 μm (**C**, **E**, **G**, **I**), and 25 μm (**D**, **F**, **H**, **J**).

Slc9a3$^{-/-}$ mice [15]. Another reason for the phenotypes may be a reduction in the epithelial surface areas available for fluid exchanges to occur, as the efferent duct is less convoluted and hypoplastic. The third reason suggested in *Lgr4*$^{-/-}$ mice is a physical blockade of the efferent ducts by immune cells; however, we did not observe such a blockade, suggesting that this possibility is not a plausible explanation in our case.

Transit through the epididymis is known to be essential for sperm maturation [35]. The spermatozoa of *Lgr4*$^{Gt/Gt}$ mice may also lack a sperm volume regulation, which was accomplished through the epididymis, as described in *Rosl*$^{-/-}$ mice [31, 36]. However, unlike the spermatozoa of *Rosl*$^{-/-}$ mice, most of the spermatozoa of *Lgr4*$^{Gt/Gt}$ mice showed a hairpin structure with tightly attached cytoplasms. In addition to the morphologic difference, we found laminin binding to the sperm surface in the cauda epididymidis of *Lgr4*$^{Gt/Gt}$ mice. All these changes could account for the infertility of *Lgr4*$^{Gt/Gt}$ mice. Taken together, the decrease of sperm motility and maturity seems to reflect the developmental defects of the epididymis in *Lgr4*$^{Gt/Gt}$ mice.

The expression of ESR1 was observed in the caput epididymidis of newborn mice of both wild-type and *Lgr4*$^{Gt/Gt}$ mice. This is consistent with the data reported by Zhou et al. [37]: ESR1 is detected in apical, narrow, and some basal cells of the initial segment; in principal cells of the caput; and in clear cells of the corpus and cauda epididymidis. In wild-type mice, the ESR1 expression gradually increases after birth and reaches a maximum level by 3 wk of age. In contrast, the ESR1 expression starts to disappear after birth in *Lgr4*$^{Gt/Gt}$ mice. On the other hand, low levels of ESR1 expression in the efferent ducts were kept constant during the postnatal development period, thereby suggesting that the regulation of ESR1 expression in the epididymis differs from that in the efferent ducts. Further investigation will be required to elucidate the role of ESR1 in the epididymis.

One surprising feature of the *Lgr4*$^{Gt/Gt}$ mouse is the lack of an initial segment in the caput epididymidis. Sonnenberg-Riethmacher et al. [24] reported that the *Rosl*$^{-/-}$ mice lacked the initial segment. *Rosl* is shown to be highly expressed in tall columnar epithelial cells of the initial segment and intermediately expressed in distally located cells of the caput, but not of the corpus or of the cauda. Our data demonstrated that *Lgr4* is mainly expressed in mesenchymal cells, but not in epithelial cells, during the postnatal development period. Altered expression of *Rosl* was not observed by the RT-PCR analysis in the epididymides of *Lgr4*$^{Gt/Gt}$ mice 1 wk of age (data not shown). It is possible that the development of initial segments requires interaction between epithelial cells and mesenchymal cells that express *Rosl* and *Lgr4*, respectively.

In addition to the lack of an initial segment, the epididymides of *Lgr4*$^{Gt/Gt}$ mice are less convoluted, suggesting a defect in the duct elongation. Well-known key molecules involved in epididymal development are steroid hormones and their receptors. Development of the male reproductive tract requires the regulation of testosterone and dihydrotestosterone through the AR. In addition to the AR and ESR1, ESR2 is expressed in the epididymis; however, we could not detect obvious differences in the expression of either AR or ESR2. Considering the data that serum concentrations of estrogen and testosterone are within normal ranges, these hormones may not be involved in the defect in the duct elongation of *Lgr4*$^{Gt/Gt}$ mice.

For elongation and convolution of the duct to occur, an extensive tissue remodeling, including cell proliferation and remodeling of the ECM, is required [38]. Mendive et al. [26] reported reduced cell proliferation in efferent ducts and in the

caput epididymidis of *Lgr4*$^{-/-}$ mice. In the present study, we found a defect in mesenchymal cell layers and in ECMs. Multilamination suggests that the defect in elongation is due to a failure in the ECM remodeling process, in addition to a reduced level of proliferation. ECM remodeling is regulated by matrix metalloproteinases (MMPs) and their tissue inhibitors (TIMPs). Some MMPs and TIMPs regulate the ureteric bud branching morphogenesis in renal development [39, 40]. In *Mpv17*$^{-/-}$ mice, the expression of MMP2 was increased [41], and an abnormal BM morphology, with transient lamination of the stria vascularis and the kidneys, was demonstrated [42]. This abnormal BM morphology is quite similar to the BMs of epididymal tubules in *Lgr4*$^{Gt/Gt}$ males. These observations suggest that the hyperactivated MMP causes the distorted BM in vivo. One abnormal BM morphology sign is an accumulation of laminin. Interestingly, an accumulation of laminin was also observed toward the mesenchymal cell layers, without the alteration of type IV collagen, in *Lgr4*$^{Gt/Gt}$ males. These facts support the notion that ECM remodeling and ECM-mediated signaling are necessary for postnatal growth and development of the epididymis. It is of interest that ECM components, including laminin-1 and type IV collagen, induce the ESR1 expression in nonmalignant mammary epithelial lines, SCp2 [43]. In addition, a reporter gene assay in SCp2 showed the regulatory element of *Esr1* promoter that responds to laminin-rich reconstituted BM [44]. Thus, the ESR1 reduction in the epididymis of *Lgr4*$^{Gt/Gt}$ males may be caused by the distorted BM structure. In addition, aberrant BM structures, together with an accumulation of testicular fluid, may cause a rupture of the tubular structure, leading to a leakage of laminin into the lumen of the epididymal ducts.

Recent studies demonstrated that the DLGR2 ligand is composed of the BMP antagonist family proteins, *burs* and *pburs* in *Drosophila melanogaster* [45, 46]; however, no homolog in mammals has yet been found. Identification of ligands for LGR4 will facilitate studies of epithelial-mesenchyme interactions, which will in turn lead to an understanding of basic principles of tubular system development.

ACKNOWLEDGMENTS

We wish to thank M. Araki, K. Haruna, T. Imamura, K. Miike, K. Miyata, Y. Sakumura, K. Semba, and Y. Tsuruta for helpful discussions and technical help and M. Nakata for excellent technical assistance.

REFERENCES

1. Hinton BT, Palladino MA, Rudolph D, Lan ZJ, Labus JC. The role of the epididymis in the protection of spermatozoa. Curr Top Dev Biol 1996; 33: 61–102.
2. Jones RC. To store or mature spermatozoa? The primary role of the epididymis. Int J Androl 1999; 22:57–67.
3. Abou-Haila A, Fain-Maurel MA. Regional differences of the proximal part of mouse epididymis: morphological and histochemical characterization. Anat Rec 1984; 209:197–208.
4. Abou-Haila A, Fain-Maurel MA. Postnatal differentiation of the enzymatic activity of the mouse epididymis. Int J Androl 1985; 8:441–458.
5. Drevet JR, Lareyre JJ, Schwaab V, Vernet P, Dufaure JP. The PEA3 protein of the Ets oncogene family is a putative transcriptional modulator of the mouse epididymis-specific glutathione peroxidase gene gpx5. Mol Reprod Dev 1998; 49:131–140.
6. Suzuki K, Lareyre JJ, Sanchez D, Gutierrez G, Araki Y, Matusik RJ, Orgebin-Crist MC. Molecular evolution of epididymal lipocalin genes localized on mouse chromosome 2. Gene 2004; 339:49–59.
7. Vernet P, Faure J, Dufaure JP, Drevet JR. Tissue and developmental distribution, dependence upon testicular factors and attachment to spermatozoa of GPX5, a murine epididymis-specific glutathione peroxidase. Mol Reprod Dev 1997; 47:87–98.
8. Hsia N, Cornwall GA. Cres2 and Cres3: new members of the cystatin-related epididymal spermatogenic subgroup of family 2 cystatins. Endocrinology 2003; 144:909–915.
9. Fox SA, Yang L, Hinton BT. Identifying putative contraceptive targets by dissecting signal transduction networks in the epididymis using an in vivo electroporation (electrotransfer) approach. Mol Cell Endocrinol 2006; 250: 196–200.
10. Ezer N, Robaire B. Gene expression is differentially regulated in the epididymis after orchidectomy. Endocrinology 2003; 144:975–988.
11. Behringer RR, Finegold MJ, Cate RL. Mullerian-inhibiting substance function during mammalian sexual development. Cell 1994; 79:415–425.
12. Yamashita S. Localization of estrogen and androgen receptors in male reproductive tissues of mice and rats. Anat Rec A Discov Mol Cell Evol Biol 2004; 279:768–778.
13. Hess RA. Estrogen in the adult male reproductive tract: a review. Reprod Biol Endocrinol 2003; 1:52.
14. Hess RA, Bunick D, Lee KH, Bahr J, Taylor JA, Korach KS, Lubahn DB. A role for oestrogens in the male reproductive system. Nature 1997; 390: 509–512.
15. Zhou Q, Clarke L, Nie R, Carnes K, Lai LW, Lien YH, Verkman A, Lubahn D, Fisher JS, Katzenellenbogen BS, Hess RA. Estrogen action and male fertility: roles of the sodium/hydrogen exchanger-3 and fluid reabsorption in reproductive tract function. Proc Natl Acad Sci U S A 2001; 98:14132–14137.
16. Krege JH, Hodgin JB, Couse JF, Enmark E, Warner M, Mahler JF, Sar M, Korach KS, Gustafsson JA, Smithies O. Generation and reproductive phenotypes of mice lacking estrogen receptor beta. Proc Natl Acad Sci U S A 1998; 95:15677–15682.
17. Couse JF, Hewitt SC, Bunch DO, Sar M, Walker VR, Davis BJ, Korach KS. Postnatal sex reversal of the ovaries in mice lacking estrogen receptors alpha and beta. Science 1999; 286:2328–2331.
18. Higgins SJ, Young P, Cunha GR. Induction of functional cytodifferentiation in the epithelium of tissue recombinants. II. Instructive induction of Wolffian duct epithelia by neonatal seminal vesicle mesenchyme. Development 1989; 106:235–250.
19. Zhao GQ, Liaw L, Hogan BL. Bone morphogenetic protein 8A plays a role in the maintenance of spermatogenesis and the integrity of the epididymis. Development 1998; 125:1103–1112.
20. Zhao GQ, Chen YX, Liu XM, Xu Z, Qi X. Mutation in Bmp7 exacerbates the phenotype of Bmp8a mutants in spermatogenesis and epididymis. Dev Biol 2001; 240:212–222.
21. Hu J, Chen YX, Wang D, Qi X, Li TG, Hao J, Mishina Y, Garbers DL, Zhao GQ. Developmental expression and function of Bmp4 in spermatogenesis and in maintaining epididymal integrity. Dev Biol 2004; 276:158–171.
22. Chen MY, Carpenter D, Zhao GQ. Expression of bone morphogenetic protein 7 in murine epididymis is developmentally regulated. Biol Reprod 1999; 60:1503–1508.
23. Liu ZZ, Wada J, Kumar A, Carone FA, Takahashi M, Kanwar YS. Comparative role of phosphotyrosine kinase domains of c-ros and c-ret protooncogenes in metanephric development with respect to growth factors and matrix morphogens. Dev Biol 1996; 178:133–148.
24. Sonnenberg-Riethmacher E, Walter B, Riethmacher D, Godecke S, Birchmeier C. The c-ros tyrosine kinase receptor controls regionalization and differentiation of epithelial cells in the epididymis. Genes Dev 1996; 10:1184–1193.
25. Mazerbourg S, Bouley DM, Sudo S, Klein CA, Zhang JV, Kawamura K, Goodrich LV, Rayburn H, Tessier-Lavigne M, Hsueh AJ. Leucine-rich repeat-containing, G protein-coupled receptor 4 null mice exhibit intrauterine growth retardation associated with embryonic and perinatal lethality. Mol Endocrinol 2004; 18:2241–2254.
26. Mendive F, Laurent P, Van Schoore G, Skarnes W, Pochet R, Vassart G. Defective postnatal development of the male reproductive tract in LGR4 knockout mice. Dev Biol 2006; 290:421–434.
27. Hsu SY. New insights into the evolution of the relaxin-LGR signaling system. Trends Endocrinol Metab 2003; 14:303–309.
28. Taniwaki T, Haruna K, Nakamura H, Sekimoto T, Oike Y, Imaizumi T, Saito F, Muta M, Soejima Y, Utoh A, Nakagata N, Araki M, et al. Characterization of an exchangeable gene trap using pU-17 carrying a stop codon-beta geo cassette. Dev Growth Differ 2005; 47:163–172.
29. Sztein JM, Farley JS, Mobraaten LE. In vitro fertilization with cryopreserved inbred mouse sperm. Biol Reprod 2000; 63:1774–1780.
30. Schoore GV, Mendive F, Pochet R, Vassart G. Expression pattern of the orphan receptor LGR4/GPR48 gene in the mouse. Histochem Cell Biol 2005; 124:35–50.
31. Avram CE, Cooper TG. Development of the caput epididymidis studied by expressed proteins (a glutamate transporter, a lipocalin and beta-

galactosidase) in the c-ros knockout and wild-type mice with prepubertally ligated efferent ducts. Cell Tissue Res 2004; 317:23–34.
32. Fouchecourt S, Lareyre JJ, Chaurand P, DaGue BB, Suzuki K, Ong DE, Olson GE, Matusik RJ, Caprioli RM, Orgebin-Crist MC. Identification, immunolocalization, regulation, and postnatal development of the lipocalin EP17 (epididymal protein of 17 kilodaltons) in the mouse and rat epididymis. Endocrinology 2003; 144:887–900.
33. Agarwal A, Hoffer AP. Ultrastructural studies on the development of the blood-epididymis barrier in immature rats. J Androl 1989; 10:425–431.
34. Timpl R, Brown JC. Supramolecular assembly of basement membranes. BioEssays 1996; 18:123–132.
35. Cooper TG. Role of the epididymis in mediating changes in the male gamete during maturation. Adv Exp Med Biol 1995; 377:87–101.
36. Yeung CH, Sonnenberg-Riethmacher E, Cooper TG. Infertile spermatozoa of c-ros tyrosine kinase receptor knockout mice show flagellar angulation and maturational defects in cell volume regulatory mechanisms. Biol Reprod 1999; 61:1062–1069.
37. Zhou Q, Nie R, Prins GS, Saunders PT, Katzenellenbogen BS, Hess RA. Localization of androgen and estrogen receptors in adult male mouse reproductive tract. J Androl 2002; 23:870–881.
38. Streuli C. Extracellular matrix remodelling and cellular differentiation. Curr Opin Cell Biol 1999; 11:634–640.
39. Pohl M, Sakurai H, Bush KT, Nigam SK. Matrix metalloproteinases and their inhibitors regulate in vitro ureteric bud branching morphogenesis. Am J Physiol Renal Physiol 2000; 279:F891–900.
40. Nee LE, McMorrow T, Campbell E, Slattery C, Ryan MP. TNF-alpha and IL-1beta-mediated regulation of MMP-9 and TIMP-1 in renal proximal tubular cells. Kidney Int 2004; 66:1376–1386.
41. zum Gottesberge AM, Felix H. Abnormal basement membrane in the inner ear and the kidney of the Mpv17−/− mouse strain: ultrastructural and immunohistochemical investigations. Histochem Cell Biol 2005; 124:507–516.
42. Reuter A, Nestl A, Zwacka RM, Tuckermann J, Waldherr R, Wagner EM, Hoyhtya M, Meyer zum Gottesberge AM, Angel P, Weiher H. Expression of the recessive glomerulosclerosis gene Mpv17 regulates MMP-2 expression in fibroblasts, the kidney, and the inner ear of mice. Mol Biol Cell 1998; 9:1675–1682.
43. Novaro V, Roskelley CD, Bissell MJ. Collagen-IV and laminin-1 regulate estrogen receptor alpha expression and function in mouse mammary epithelial cells. J Cell Sci 2003; 116:2975–2986.
44. Novaro V, Radisky DC, Ramos Castro NE, Weisz A, Bissell MJ. Malignant mammary cells acquire independence from extracellular context for regulation of estrogen receptor alpha. Clin Cancer Res 2004; 10:402S–409S.
45. Mendive FM, Van Loy T, Claeysen S, Poels J, Williamson M, Hauser F, Grimmelikhuijzen CJ, Vassart G, Vanden Broeck J. *Drosophila* molting neurohormone bursicon is a heterodimer and the natural agonist of the orphan receptor DLGR2. FEBS Lett 2005; 579:2171–2176.
46. Luo CW, Dewey EM, Sudo S, Ewer J, Hsu SY, Honegger HW, Hsueh AJ. Bursicon, the insect cuticle-hardening hormone, is a heterodimeric cystine knot protein that activates G protein-coupled receptor LGR2. Proc Natl Acad Sci U S A 2005; 102:2820–2825.

International weekly journal of science

nature

Suppression of basal autophagy in neural cells causes neurodegenerative disease in mice

Taichi Hara[1], Kenji Nakamura[2], Makoto Matsui[1,3,4], Akitsugu Yamamoto[5], Yohko Nakahara[2], Rika Suzuki-Migishima[2], Minesuke Yokoyama[6], Kenji Mishima[7], Ichiro Saito[7], Hideyuki Okano[8,9] & Noboru Mizushima[1,10]

[1]Department of Bioregulation and Metabolism, Tokyo Metropolitan Institute of Medical Science, Tokyo 113-8613, Japan. [2]Mouse Genome Technology Laboratory, Mitsubishi Kagaku Institute of Life Sciences, Tokyo 194-8511, Japan. [3]Department of Basic Biology, School of Life Science, the Graduate University for Advanced Studies, Okazaki 444-8585, Japan. [4]Department of Cell Biology, National Institute for Basic Biology, Okazaki 444-8585, Japan. [5]Department of Bio-Science, Nagahama Institute of Bio-Science and Technology, Nagahama 526-0829, Japan. [6]Brain Research Institute, Niigata University, Niigata 951-8510, Japan. [7]Department of Pathology, Tsurumi University School of Dental Medicine, Yokohama 230-8501, Japan. [8]Department of Physiology, Keio University School of Medicine, Tokyo 160-8582, Japan. [9]SORST and [10]PRESTO, Japan Science and Technology Agency, Kawaguchi 332-0012, Japan.

Reprinted from Nature, Vol. 441, No. 7095, pp. 885-889, 15 June 2006